M 2016

U.PORTO
FEUP FACULDADE DE ENGENHARIA
UNIVERSIDADE DO PORTO

KNEE SIMULATION SYSTEM TO PREVENT INJURIES IN VOLLEYBALL ATHLETES

JOÃO CUNHA

DISSERTAÇÃO DE MESTRADO APRESENTADA
À FACULDADE DE ENGENHARIA DA UNIVERSIDADE DO PORTO EM
ENGENHARIA BIOMÉDICA

U.PORTO
FEUP FACULDADE DE ENGENHARIA UNIVERSIDADE DO PORTO

MEB - MESTRADO EM ENGENHARIA BIOMÉDICA **2015/2016**

A Dissertação intitulada

"Knee Simulation System to Prevent Injuries in Volleyball Athletes"

foi aprovada em provas realizadas em 19-07-2016

o júri

Presidente Prof. Doutor João Manuel Ribeiro da Silva Tavares
Professor Associado c/ Agregação do Departamento de Engenharia Mecânica da FEUP - U.Porto

Prof.ª Doutora Isabel Maria Pereira Leite de Freitas Loureiro
Professora Auxiliar Convidada da Escola de Engenharia da U. Minho

Prof. Doutor Miguel Fernando Paiva Velhote Correia
Professor Auxiliar do Departamento de Engenharia Eletrotécnica e de Computadores da FEUP - U. Porto

O autor declara que a presente dissertação (ou relatório de projeto) é da sua exclusiva autoria e foi escrita sem qualquer apoio externo não explicitamente autorizado. Os resultados, ideias, parágrafos, ou outros extratos tomados de ou inspirados em trabalhos de outros autores, e demais referências bibliográficas usadas, são corretamente citados.

Autor - João Miguel de Oliveira Ferreira da Cunha

Faculdade de Engenharia da Universidade do Porto

FACULDADE DE ENGENHARIA DA UNIVERSIDADE DO PORTO

Knee simulation system to prevent injuries in volleyball athletes

João Cunha

DISSERTATION

Master degree in Biomedical Engineering

Supervisor: Professor Miguel Velhote Correia

Second Supervisor: Professor Abel Rouboa

July 26, 2016

© João Cunha, 2015

Knee simulation system to prevent injuries in volleyball athletes

João Cunha

Master degree in Biomedical Engineering

July 26, 2016

Resumo

Lesões no ligamento cruzado anterior (ACL) e ao nível patelofemoral têm grande impacto em atletas femininas federadas e profissionais. Particularmente em atletas de voleibol, a incidência em lesões ao nível do joelho relativamente aos movimentos de salto e queda, são maiores nas mulheres em comparação com os homens.

Este estudo consistiu na investigação dos efeitos que os incrementos em altura em drop jumps têm nos parâmetros neuromusculares, cinemáticos e cinéticos numa atleta feminina federada. Além disso, foram alterados os parâmetros musculares do modelo musculoesquelético, de forma a ser possível comparar atletas lesionados e saudáveis.

A aquisição do movimento humano relativo aos drop jumps e os dados electromiográficos dos músculos quadríceps, isquitobiais e gastocnemius foi comparada com os valores da simulação numérica. Para aspectos de analise foi apenas considerada a fase de queda, uma vez que é a mais suscetível a lesão. Um modelo musculoesquelético foi desenvolvido com o foco no joelho, dado que os modelos standard disponíveis não incluem patela, tendão patelar e ACL. Assim, a articulação do joelho está mais próxima das caraterísticas anatómicas.

Os passos usados na simulação numérica consistiram no Scaling, Algoritmo de remoção de residuais (RRA) e Optimização estática. Através destas ferramentas de simulação foi possível estimar as ativações e forças musculares. Além disso, parâmetros do ACL como cumprimento das fibras e energia absorvida, momentos Tibiofemorais (TF) e Patelofemorais (PF) foram também estimados.

Os resultados obtidos demonstraram que o drop jump a 45 cm de altura foi o salto com maior risco, apresentando maior adução da anca combinado com valgus do joelho. Relativamente à comparação do atleta lesionado e saudável, o lesionado apresentou maior ativação dos quadríceps e défice de força muscular, o que poderá traduzir mais esforço sobre o ACL e distúrbios patelares.

Em suma, este estudo deu origem a informação estimada numericamente que poderá ser bastante benéfica na prevenção de lesões no ACL e PF. Baseado nesta informação será possível estabelecer programas de prevenção, de forma a assegurar a prática segura por parte dos atletas.

Abstract

Anterior cruciate ligament (ACL) and patellofemoral (PF) injuries have high impact in female recreational and professional athletes. In particular, volleyball female athletes have more incidence of knee injures in jumping and landing tasks in comparison with male athletes.

This study investigated effects of increasing drop jump heights on neuromuscular, kinematic and kinetic properties of the knee in one female recreational athlete. Furthermore, some muscular parameters of the musculoskeletal model were modified, in order to match the anthropometry of an injured athlete. In this way, it was possible to compare healthy and injured athletes in drop jump tasks.

Motion capture data was obtained from drop jump trials and electromyography (EMG) data collected from hamstrings, gastrocnemius and quadriceps which were then compared to numerical estimated activations. For analysis purposes it was selected only the landing phase which is considered the most common phase for an injury to occur. A musculoskeletal model was designed with major focus on the knee joint, since standard models do not include the patella, patellar tendon and ACL ligament. Hence, knee joint definition is proximal to the anatomical characteristics.

Numerical simulation tools used were Scaling, Residual reduction algorithm (RRA) and Static optimization. Through these tools muscle activation and forces were computed. In addition, ACL fibre length, ACL power, Tibiofemoral (TF) moments and Patellofemoral (PF) moments were also computed.

Results showed that drop jump at 45 cm of height was the most dangerous trial, in which higher hip adduction coupled with knee valgus were verified. Moreover, and regarding to the comparison between healthy and injured, injured athletes showed higher quadriceps activations and muscle weakness which may traduce ACL strain and patellar disorders.

In summary, this work provide some numerical estimation informations that could be helpful for ACL and PF injury prevention. Based on this information preventive programmes may be formulated in such way that athletes could practice sports safely.

Acknowledgements

First, I am deeply grateful to my supervisors Prof. Miguel Velhote Correia and Prof. Abel Rouboa for helping me whenever I need and for sharing their knowledge and experience with me.

Secondly, I want to thank to Carlos Rodrigues all the support and guidance that he gave me during this work. Moreover, I want o thank to Dra.Marta Massada all the kindness, sympathy and medical support, and to Pedro Fonseca for his help in the experimental trials and availability for my doubts.

Finally, I must thank my family, friends, and my girlfriend for giving me the encouragement and support specially in the tough times.

João Cunha

"Ambition is the path to success.
Persistence is the vehicle you arrive in "

Bill Bradley

Contents

List of Figures

List of Tables

List of Abbreviations

3D	Three dimensional
ACL	Anterior cruciate ligament
AM	Anteromedial
COM	Centre of mass
CT	Computerized tomography
DOF	Degrees of freedom
EMG	Electromyography
G:Q	Gastrocnemius to Quadriceps
H:Q	Harmstrings to Quadriceps
IK	Inverse Kinematics
IMUs	Inertial measurement units
MEMS	Miniature or micro-electromechanical systems
MRI	Magnetic resonance imaging
MVC	Maximum voluntary contraction
PCA	Posterior cruciate ligament
PM	Posterolateral
PF	Patellofemoral
RRA	Residual reduction algorithm
sEMG	Surface EMG
TF	Tibiofemoral

Chapter 1

Introduction

Volleyball has become an extremely popular participation sport worldwide. According to the International Volleyball Federation, FIVB, approximately 800 million athletes practice this sport which make it one of the world's most popular (Reeser and Bahr, 2011).

Injuries are a common and unfortunate scenario that affects many volleyball athletes that are associated to diverse factors. Such as gender, duration of training and competition, as well as anthropometric and physical characteristics (Cassell, 2001). Most concretely, in volleyball game, lower limbs injuries are more common with major incidence at knee level (Reeser and Bahr, 2011). Knee ligament rupture, patellar tendinitis and patellofemoral abnormal tracking are the most commonly injuries in volleyball environment (Ferretti et al., 1992; Briner and Kacmar, 1997). Although it should be noted that volleyball athletes are at risk of other injuries, including lower back pain, finger sprains, contusions and abrasions (Reeser and Bahr, 2011).

Monitoring knee activity is essential to understand how it will be possible to predict injuries affecting volleyball players. To monitor these injuries it is necessary to use systems that are able to collect valid data from the knee, without compromising the athlete's mobility. In recent decades, ambulatory systems using miniature or micro-electromechanical systems (MEMS) inertial sensors started to be proposed to monitor aspects of motor function in healthy subjects and patients in sports natural environment (van den Noort et al., 2013; Favre et al., 2009; Feldhege et al., 2015). The gold standard of these devices are the inertial measurement units (IMUs), that are composed by three dimensional 3D rate gyroscopes and 3D accelerometers (Seel et al., 2014).

Experimental data by itself is not sufficient to extract important variables to predict knee injuries, since variables as the forces generated by the muscles are not generally measurable in experiments(Delp et al., 2007; Kar and Quesada, 2012). For that reason, it is important to use simulations to study and estimate internal loading of the musculoskeletal system, and neuromuscular coordination (Delp et al., 2007). Most importantly, the ability to simulate a specific injury makes possible to extract important information about how this injury occurs. Indeed, the combination of simulation tools and experimental data it is a accurate and strong way that could prevent injuries scenarios. Moreover, could help athletes to improve their performance and training techniques (Delp et al., 2007; Seth et al., 2011).

1.1 Motivation

The continuous increasing of knee injuries in sports is a common scenario that are presented in athletes careers. By this way, there is a need to help them to reduce the appearance of these injuries. Image-based techniques as X-rays, computerized tomography (CT) and magnetic resonance imaging (MRI) are the common diagnostic tools to asses knee joint condition. However, these tools can not be used in sport game environment. Indeed, a novel method is needed to monitoring knee joint in a way that allows the mobility of the athletes, but at the same time, extract important data to prevent a possible injury.

1.2 Aim

The aim of this dissertation consists in the development of a methodology that allows to assess knee joint effort in volleyball game movements. This may have potential applications in personalised training plans and injury prevention. By this way, through a combination of devices and techniques, as human motion trackers, electromyography and simulations tools it will be possible to make a precise and personalised analysis of knee joint efforts.

To achieve this goal, the following objectives were defined:

- Evaluation of drop jump effects in knee joint for specific cases
- Development of personalised biomechanical model to include patella, patellar tendon and ACL
- Identification of changes to musculoskeletal parameters that characterise an injured athlete
- Identification of injury risk patterns
- Provision of relevant information to suggest preventive training programs

1.3 Structure

This report was organized in different chapters. Chapter 1 introduces the dissertation focus. In chapter 2 the background and all the theory fundamentals applied on this work were explained. Chapter 3 is relative to the materials and methods and chapter 4 to the obtained results and its discussion. At least, chapter 5 is relative to the conclusions and future work.

Chapter 2

Background and theory fundamentals

The knee joint is an incredibly strong, intricate and complex part of human anatomy. In order to evaluate how knee volleyball injuries occur, it is essential to understand the anatomical aspects related to knee joint functioning. For that, it is necessary to explore the main components of knee joint.

Moreover, it is important to understand all the theory fundamentals that are associated to simulation methodologies, as well as, the experimental setup that was used to acquire the kinematic and kinetic data.

In this chapter, a general background of knee joint anatomy, knee volleyball injuries was presented. Furthermore, kinematic and kinetic of human motion approaches were evaluated. It was also explained every step of simulation used in this work.

2.1 Knee joint

Knee joint it is the largest and one of most important joints in the human body (Fig 2.1). Its role is to provide strength, support, and flexibility while standing, walking, running and sitting. To a better understanding, joint concept is related to a place where two bones or more come together allowing movement and providing support. As the knee is a synovial hinge joint, its function is to permit the flexion and extension of the lower leg relative to the thigh (Seeley et al., 2005; Taylor, 2015). Oily synovial fluid is produced by the synovial membrane that lines the joint capsule and fills the hollow space between the bones, lubricating the knee to reduce friction and wear (Seeley et al., 2005; Taylor, 2015).

Functionally, the knee comprises two articulations, the patellofemoral and tibiofemoral. The tibiofemoral articulation is a condylar joint formed between three bones (femur, tibia and patella), whereas the patellofemoral articulation is a gliding joint (Kreder and Hawker, 2010). The tibiofemoral joint allows transmission of body weight from the femur to the tibia while providing hinge-like, sagittal plane joint rotation along with a small degree of tibial axial rotation (Flandry and Hommel, 2011). In other hand, patellofemoral articulation in addition with quadriceps muscle group act to dissipate forward momentum as the body enters the stance phase of gait cycle (Flandry and

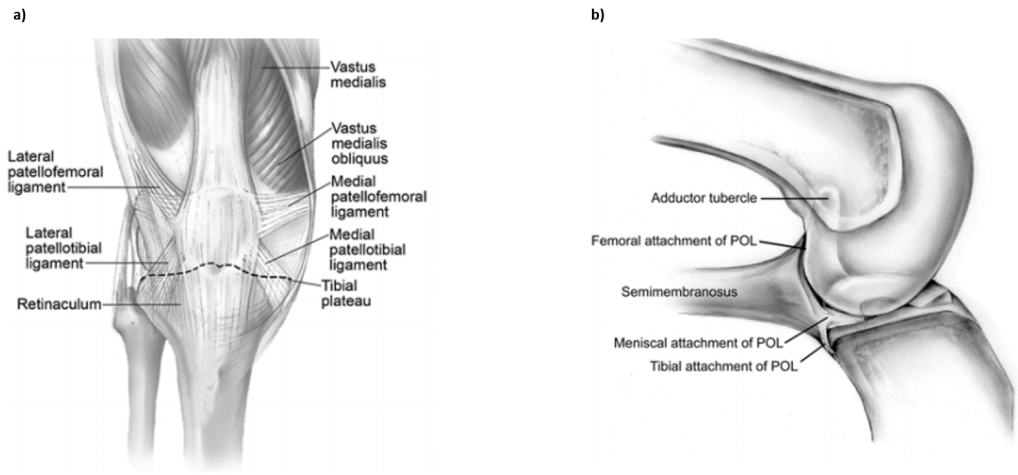

Figure 2.1: a) Ligaments and muscle of knee joint. b) Femur and tibia connection supported by menisci cartilage (Flandry and Hommel, 2011).

Hommel, 2011).

In terms of stability, this joint is governed by a combination of static ligaments, dynamic muscular forces, meniscocapsular aponeurosis, bony topography, and joint load (Flandry and Hommel, 2011).

2.1.1 Bones and ligaments

Beyond femur and tibia knee joint is composed by other bones as the patella and trochlea. The patella is the largest sesamoid bone in the body. It resides within the trochlear groove of the distal femur and links the extensor mechanism through connections to the quadriceps tendon at its superior pole and the patellar tendon at its inferior pole (Sherman et al., 2014). At least, the trochlea is formed by the anterior aspect of the distal femur and has a centralized trochlear groove with associated medial and lateral facets (Sherman et al., 2014). The condyles help to stabilize the patella, preventing lateral translation (Thomas et al., 2014).

In terms of ligaments, it is important to mention capsular, cruciate and collateral ligaments. Capsular ligaments compose the static tibiofemoral ligaments and are involved in tibiofemoral stability (Flandry and Hommel, 2011). Together, these structures cup and buttress the posterior aspect of the femoral condyles accommodating their increasing volume in knee extension and decreasing volume in knee flexion (Flandry and Hommel, 2011). Relative to cruciate ligaments these are divided in anterior and posterior cruciate ligaments. The first one plays an important role in preventing the hyperextension of the knee by limiting the anterior movement of the tibia (Seeley et al., 2005). The second one prevents the posterior movement of the tibia relative to the

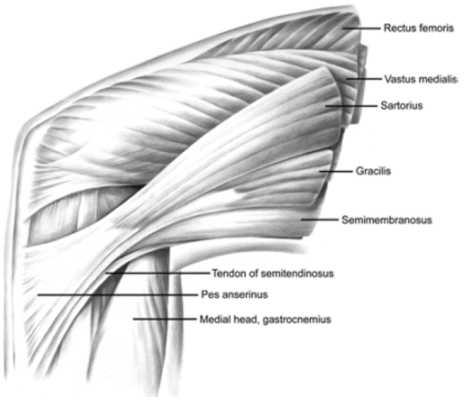

Figure 2.2: Knee flexors and extensors muscles (Flandry and Hommel, 2011).

femur (Seeley et al., 2005). Moreover, collateral ligaments stabilize the medial and lateral sides of the knee (Seeley et al., 2005).

2.1.2 Muscle and Tendons

Muscles are important structures for knee flexion and extension movement. They are attached to the femur, tibia, and fibula through the ligaments (Seeley et al., 2005). The quadriceps is the sole muscle group that crosses the patellofemoral joint, making it the primary contributor of the knee extensor mechanism (Shalhoub and Maletsky, 2014). It is formed by the convergence of four muscles represented in figure 2.2: the rectus femoris, vastus medialis, vastus lateralis, and vastus intermedius (Sherman et al., 2014). In other hand, knee flexor mechanism is composed by seven muscles: semi-tendinosis, semi-membranosis, biceps femoris, sartorius, gracilis, popliteus and gastrocnemius. Although the main function of these muscles is knee flexion, some muscles performs knee internal (semi-tendinosis, semi-membranosis, popliteus) and external (biceps femoris,sartorius) rotations (Flandry and Hommel, 2011).

Tendons are elastic tissue that technically compose part of the muscles and connect them to the bones (Seeley et al., 2005). There are two main tendons in the knee: patellar and quadriceps tendons. The patellar tendon is the continuation of the quadriceps tendon, composed mostly of the rectus femoris component passing over the anterior aspect of the patella, and inserts on the tibial tubercle (Thomas et al., 2014). The quadriceps tendon is the common tendon formed between the myofascial junctions of the superficial layer of the rectus femoris muscle, the middle layers of the vastus medialis and vastus lateralis muscles, and the deep layer of the vastus intermedius muscle

(Thomas et al., 2014). Biomechanically, the quadriceps tendon and the patella are integral parts of the active and passive extensor mechanisms of the knee joint (Thomas et al., 2014).

2.1.3 Knee cartilage

Cartilage tissue at knee joint is composed from two different types: menisci and articular cartilage. Articular cartilage is a white, smooth, fibrous connective tissue that covers the ends of bones and protects the bones as the joint moves (Sherman et al., 2014). The articular cartilages of the knee cover the ends of the femur, the top of the tibia and the back of the patella (Sherman et al., 2014). This characteristics allow that bones move against each other easily and without pain. Characterized as complex anatomy, menisci serve a variety of biomechanical functions such as load bearing, constituting a contact area, guiding rotation, and stabilizing translation (Flandry and Hommel, 2011). It is composed in two parts, medial and lateral menisci. Once the menisci are shaped like a shallow socket to accommodate the end of the femur, they help the ligaments in making the knee stable (Flandry and Hommel, 2011).

2.2 Voleyball knee injuries

Although volleyball be a non-contact game in which players of opposing teams are separated by a net, there a prevalence of some injuries. This sport involves rapid and forceful movements that contribute for the appearance of these injuries (Ferretti et al., 1992). The most usual at knee level are patellofemoral abnormal tracking, and ligament injuries (Ferretti et al., 1992; Briner and Kacmar, 1997).

2.2.1 Patellofemoral abnormal tracking

Patellofemoral abnormal tracking is one of the most common knee dysfunctions with high prevalence (25%) in general population (Wilson et al., 2009). This disease can be defined as movement of the patella out of its normal position (Golant et al., 2013). A large spectrum of disease including patellofemoral pain, instability, focal chondral disease, and arthritis are associated to this disorder (Sherman et al., 2014).

In normal patellar tracking, illustrated in figure 2.3 a), the patella acts to magnify either force or displacement, depending on the activity, and helps to increase the moment arm of the quadriceps (Thomas et al., 2014). When the knee begins to flex, a medial patellar shift is produced and the patella stays centred as it engages the trochlear groove (Sherman et al., 2014). As flexion increases the contact area of the patella increases, and moves from distal to proximal in femur direction. Once the knee flexes past 90 degrees the quadriceps tendon contacts the trochlea and absorbs some of the joint reaction force (Sherman et al., 2014). Between 90 and 135 degrees of knee flexion, the patella rotates, and the ridge that divides the medial and odd facets engages the femoral condyle (Sherman et al., 2014). In full extension the patella remains in a slightly lateralized position (Wilson et al., 2009; Sherman et al., 2014) . However, abnormal tracking

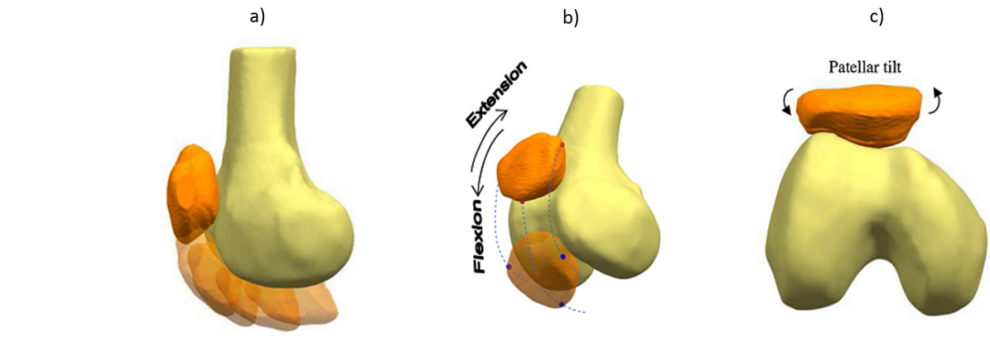

Figure 2.3: a) Patellofemoral joint simulation in different angles. b) Patellar tracking throughout knee flexion and extension movement. c) Patellar tilt (Yu and Sun, 2014).

is characterised as a different scenario in which lateral patellar translation and spin are presence (Wilson et al., 2009). In addition, abnormal central tracking within a normal trochlear groove and patellar tilt are other factors of abnormal patellar tracking (Wilson et al., 2009; Sherman et al., 2014). This phenomenon is described is figure 2.3c)

Indeed, some anatomic abnormalities could be responsible to this disorder. Weakness of the vastus medialis oblique may cause the patella to shift and rotate laterally during knee flexion (Wilson et al., 2009). Furthermore trochlear dysplasia, patella alta or baja, absence of static medial soft tissue restraints and tibial tubercle position predisposes the patient to this biomechanical abnormality(Sherman et al., 2014).

Actually, a variate clinical procedures represented in table 2.1 are used to detect Patelofemoral abnormal tracking. Moreover other solutions as electromagnetic sensors, three dimensional (3D) video analysis markers, goniometers, coordinate measuring machines and clamping techniques are used to evaluate patellar tracking (Bey et al., 2008; Wilson et al., 2009).

2.2.2 Knee ligament injuries

Knee ligament injuries is other injury that affects volleyball players with major incidence in female athletes (80% vs 20%) (Fulkenson, 2004; Zahradnik et al., 2014; Nyman and Armstrong, 2015). Anatomical different structures and hormonal behaviour could be the reason for such difference (Cassell, 2001). The most reported cases in the literature correspond to anterior cruciate ligament (ACL) injury (Ferretti et al., 1992; Zahradnik et al., 2014). ACL injury is a serious and common problem in volleyball with an incidence of ACL rupture as two injured athletes per 100,000 athletes

Table 2.1: Current diagnostic procedures (Thomas et al., 2014; Wilson et al., 2009; Golant et al., 2013; Fulkenson, 2004).

Method	State	Advantages	Disadvantages
Q-angle	Dynamic and static	Malalignment that increases the Q-angle increases the laterally-directed forces,and thus predisposes to patellofemoral instability	Indirect measurements.
Fluoroscopy	Dynamic and static	Reasonable levels of theoretical accuracy. Dynamic approach	Exposure to ionizing radiation. Abnormal motion.
Radiography	Static	Evaluation of PF articulation, morphology of patella, size of the patella with respect to the trochlea.	Only static movements. Distortion of the patella with the patient prone. Lack of adequate visualization.
CT	Static	Useful for assessing bony anatomy and malalignment	High exposure to radiation. Limited scanning plane. Alteration of the image by artefacts.
MRI	Static	Very useful for identifying articular cartilage damage and osteochondral fragments.	Long imaging times. Require the patient to contract, the quadriceps muscle for long periods, and they cannot evaluate functional tasks during full weight-bearing.
Ultrasound	Static and dynamic	Accuracy and predictive value in identifying the location and severity of the medial patellofemoral ligament.	Limited depth of penetration, lack of penetration of bone.

during one hour in male volleyball (Zahradnik et al., 2014).

Biomechanically, the most common injury scenario is characterised by rapid changes of direction, sudden deceleration, high ground reaction forces, rapid loading times and landing from a jump (Zahradnik et al., 2014; Nyman and Armstrong, 2015). Ferretti et al. (1992) reported that the most frequent mechanism of injury in volleyball was landing from a jump in the attack zone. In this characteristic movement, when the athlete contacts with the ground, a combination of valgus loading with either knee internal rotation or external rotation moments increases the tensile force in the ACL (Zahradnik et al., 2014). Moreover, deficits in knee flexion and low knee separation distance during the first 40 ms following initial ground contact increases the predisposition for ACL injury (Nyman and Armstrong, 2015).

ACL tears and injuries in menisci cartilages are the consequence of the previous related factors (Briner and Kacmar, 1997). The first one has greater incidence and is related to partial or complete disruption of the ligament tissue (Zahradnik et al., 2014; Briner and Kacmar, 1997).

Energy absorption by leg muscles during landing are an important issue that are associated to ACL prevention (Zahradnik et al., 2014; Nyman and Armstrong, 2015). This factor may reduce the amount of energy transferred to the capsule-ligamentous (Zahradnik et al., 2014). Neuromuscular training begins to emerge as a solution for real-time feedback training for improving bilateral peak knee flexion angle and peak knee separation distance in drop jumps landings (Nyman and

Armstrong, 2015).

2.2.3 Risk factors

Excessive hip adduction coupled with knee valgus, internal rotaion and low flexion angle is a risk factor that are associated to ACL injury and patellofemoral dysfunction (Hewett et al., 2005a; Dai et al., 2014). One of the causes for this phenomenon is related to hip muscles strength reduction (Powers, 2010). Muscle activation decrease relative to medial quadriceps and hamstrings are associated to an increase in knee valgus (Harput et al., 2014). Patellar maltracking is commonly associated to the atrophy of vastus medialis obliquus. It was been demonstrated by (Pal et al., 2014) that patients with patellar maltracking correlates with a delayed activation of the vastus medialis obliquus. As consequence, knee valgus influence the patella tracking leading to a lateralization of the patella (Petersen et al., 2014).

2.3 Kinematics

Kinematics consists in the study of human motion without considering the presence of forces that cause the movement. Through this analysis it is possible to quantify the role of movement between segments and joints. These two properties are considered a system of particles that form a rigid body with the ability of both translational and rotational motion (Chèze, 1984; Shull et al., 2014). By other hand, kinematics also allows the study of the velocities, accelerations and positions of this rigid body (Heintz, 2006).

An important role is to define the different joint actions that result from different types of human movement or motion. To a better understanding, figure 2.4, represents the different axes that represent human global reference system (Chèze, 1984). This reference system is useful to identify the anatomical planes and axes of motion.

2.4 Joint and segment Kinematics

Human joints are composed by the connection of two different body segments as femur, ankle, tibia, foot, pelvis and others. The joint definition is based on distal and proximal body segments, being that, distal segment is closest from the ground. By this way, joint motion is defined as the motion of the distal segment relative to the proximal one (Chèze, 1984; Hicks, 2012). According to the motion performed, these two rigid body segments attached in a certain joint change.

As mentioned before this kind of joint can perform rotational and translational movements. Considering just rotational movements, these could be characterised as the motion around the three dimensional coordinate system. Cardan sequence of rotation which is widely used in Biomechanics, describes the sequence of rotation of the different axis rotate about (Chèze, 1984; Cole et al., 1993; Heintz, 2006). The first rotation, θ_1, is relative to $X^{'}$ axis to get $X^{'}$, $Y^{'}$, $Z^{'}$; the second rotation, θ_2 ,is relative to $Y^{'}$ to get $X^{''}$, $Y^{''}$, $Z^{''}$; the third rotation,θ_3, is relative to $Z^{'}$ to get $X^{'''}$, $Y^{'''}$, $Z^{'''}$ (Heintz, 2006); These rotations could be written trough the 3x3 following matrix (Kar, 2011):

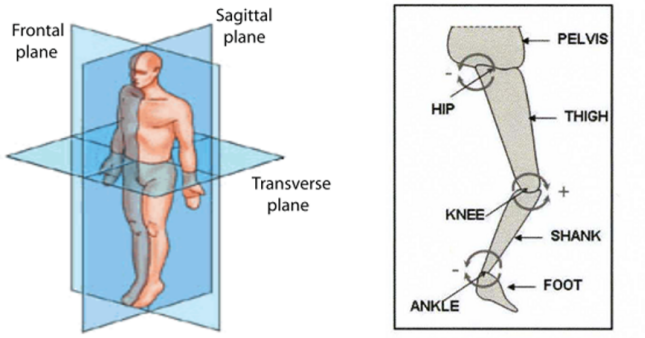

Figure 2.4: a) Orientation of the global reference coordinates system (GCS); b) Moments at lower limb joints (Kar, 2011).

$$\begin{bmatrix} X'' \\ Y'' \\ Z'' \end{bmatrix} = \begin{bmatrix} c(\theta_3)c(\theta_2) & s(\theta_1)s(\theta_3)c(\theta_2)+c(\theta_1)c(\theta_2) & -c(\theta_1)s(\theta_3)c(\theta_2)+s(\theta_1)s(\theta_2) \\ -c(\theta_3)c(\theta_2) & -s(\theta_1)s(\theta_3)c(\theta_2)+c(\theta_1)c(\theta_2) & c(\theta_1)s(\theta_3)c(\theta_2)+s(\theta_1)s(\theta_2) \\ s(\theta_3) & -s(\theta_1)c(\theta_3) & c(\theta_1)c(\theta_3) \end{bmatrix} = \begin{bmatrix} X' \\ Y' \\ Z' \end{bmatrix} \tag{2.1}$$

where the proximal [X',Y',Z'] coordinate system is rotated into the distal [X",Y",Z"] coordinate system. In this way, the three rotational motion angles are identified. Motion defined as flexion and extension occurs around the transversal axes(y-z plane), abduction (moving out from the body) and adduction (toward the body) occurs around anteroposterior axes (x-z plane) and at least, internal and external rotations occurs around longitudinal axes (x-y plane) (Cole et al., 1993).

2.5 Kinetics

Kinetics examine the forces that act on human body. Knowledge about this forces is important to understand their influence in human movement. Internal forces are related to joint contact forces, muscle, tendon and ligament activity (Godfrey et al., 2008; Seth et al., 2011). External forces consists in ground reaction forces, applied forces to musculoskeletal system and segment weight (Heintz, 2006).

Kinetic forces and moment on the joints, consists in the summation of the external forces such as gravitational and ground reaction forces in addition with, internal forces and moments applied by the muscles, ligaments and tendon in the distal and proximal segments. This approach is based on Newton's second law of motion and Euler dynamic equation (Heintz, 2006):

$$R = ma$$
$$M = I\alpha \tag{2.2}$$

where m is the mass of the object, a is the linear acceleration, I, is the mass moment of inertia, α is the angular acceleration. M and R, correspond to the muscle moments and reaction forces, respectively.

2.6 Inverse dynamics

Inverse dynamic analysis is a method for computing the net joint moments, net joint powers and intersegmental forces through kinematic motion and inertial properties (Heintz, 2006; Hicks, 2012). These approach relies in solving Newton's second law described in equation 2.3 across the human body segments (Bisseling and Hof, 2006; Vlietstra, 2014). Generally, this evaluation starts at foot segment with the ankle joint forces and moments, and progress segment by segment, using the results of the previous segment (Bisseling and Hof, 2006; Vlietstra, 2014).

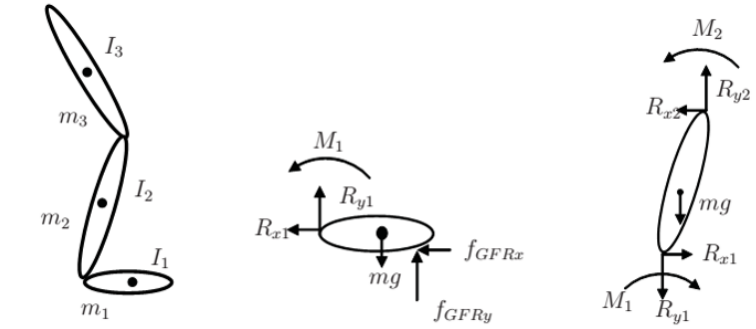

(a) Link segment (b) Foot segment (c) Shank segment

Figure 2.5: Lower limbs body segments moments of inertia, reaction forces, masses and joint moments (Heintz, 2006).

Defining the forces in the y direction the moment relative to the proximal joint to the ground (ankle) could be describe as M1 (Heintz, 2006; Bisseling and Hof, 2006):

$$\sum R_{y1} = m_1 a_{y1} = f_{GRFy1} + R_{y1} - mg$$
$$\sum M_1 = I\alpha = f_{GRFy1} d_{GRFy1} + R_{y1} d_{y1} + M_1 \tag{2.3}$$

where d_{y1} describe the moment arm to the reaction force R_{y1} to the ankle joint , d_{GRFy1} describe the moment arm to the ground reaction force f_{GRFy1} to the ankle joint. Through kinematic data it is possible to extract linear and angular acceleration, a and α respectively. Each bone segment associated to a joint has a certain weight, described as mg and located at the centre of mass (COM). Moment of inertia, I, is evaluated from anthropometric tables available in the literature. According with Newton's third law, there is an opposite and equal force at each joint (Bisseling

and Hof, 2006). In this way, knee joint moment and forces are obtained applying opposite and equal reaction force on the shank segment (Heintz, 2006; Bisseling and Hof, 2006).

It is important to understand that, inverse dynamics approach does not provide information about the contribution of individual muscles (Bisseling and Hof, 2006; Vlietstra, 2014). For instance, a net moment could be evaluated from a single antagonistic muscle or from two muscle, one antagonistic and other agonist.

2.7 Electromyography

Muscle contractions is described as an electrical response of muscles to the excitations provided by the central nervous system. Electromyography is a quantification method of these electrical signals that are associated to muscle activations (Merletti and Parker, 2004). Furthermore, electromyographic signal allows to collect information relative to intervals of muscle activity, muscle fatigue and intensity of muscle activation (Merletti and Parker, 2004; Farfán et al., 2010; Jamal, 2012).

Generally there are two types of EMG, surface and intramuscular EMG. Surface EMG (sEMG) and intramuscular EMG signals are recorded by non-invasive and invasive electrodes respectively. Due to the invasive characteristic, sEMG is widely used by the research community. However several signal contaminations are verified in this approach. Electrical noise and biological biases as skin artefacts and muscle cross-talk are the most common (Merletti and Parker, 2004; Farfán et al., 2010). By this way, it is essential to use processing techniques to attenuate these biases. Information relative to EMG data acquisition and processing used in this thesis is described in the chapter 3.

2.7.1 Surface EMG Electrodes placement and types

Surface EMG electrodes are structures that provide a simple and non-invasive measurement of EMG signals (Jamal, 2012). There are two types of electrodes: gelled and dry electrodes Merletti and Parker (2004); Farfán et al. (2010).

Beginning in the gelled electrodes, these are characterised by an interface between them and the skin. Gelled electric substance assures this interface and increases the signal acquisition accuracy. Other important part of these electrodes is the metal junctions where oxidation and reduction reactions take place (Merletti and Parker, 2004; Jamal, 2012). Silver- silver chloride (Ag-AgCl) is the commonly used composites for the metallic part of gelled electrodes. As advantage AgCl layer increases the acquisition of the muscle potential across the junction between the electrolyte and the electrode (Farfán et al., 2010; Jamal, 2012). Compared with equivalent metallic electrodes (Ag) these introduces less electrical noise into the measurement (Farfán et al., 2010).

In contrast, dry electrodes do not use a gel interface between the detection surface and the skin. Array and bar electrodes are examples of dry electrodes (Jamal, 2012). These electrodes are characterised by multiple detecting surfaces.

Electrodes placement is an important topic of EMG, once this placement could affect the acquired signal. In this way, a correct location of electrodes should be assured. For a good extraction of EMG signal, the electrode should be placed between the motor unit and tendinous insertion of the muscles (Merletti and Parker, 2004; Jamal, 2012). Moreover, the longitudinal axis of the electrode should be parallel relative to the directions of muscles fibres as illustrated in the figure 2.6. Other important concern is skin preparation. This procedure is important to reduce the skin

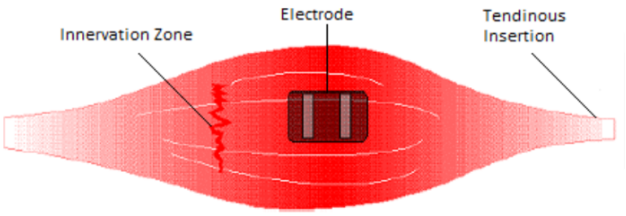

Figure 2.6: Electrodes ideal placement along the muscles (Jamal, 2012).

impedance, in order to acquire a good EMG signal. Usually an abrasive gel is used to reduce the dry layer of the skin (Jamal, 2012).

2.7.2 EMG filtering

Butterworth digital filters are often used to smooth biomechanical data, such as EMG signal. Band pass, low pass and high pass Butterworth digital filters could be applied. Basically, these filters are sophisticated moving average filters with optimally flat in their pass-band response (Robertson and Dowling, 2003).

Applying these filters to the raw EMG signal it is possible to smooth high and low frequencies components that contaminate the signal. Butterworth filter frequency response is defined as a "Maximally flat" once the pass band response is characterised as flat as between 0 Hz (DC) until the cut off frequency (Basic Electronics Tutorials, 2015). Indeed and in accordance in the figure 2.7, the higher the Butterworth filter order, the closer the filter becomes to the ideal "Brick wall" response (Basic Electronics Tutorials, 2015).

In equation 2.4 is represented the frequency response related to the Butterworth filter order (Robertson and Dowling, 2003; Basic Electronics Tutorials, 2015):

$$H_{(j\omega)} = \frac{1}{\sqrt{1+\varepsilon^2\left(\frac{\omega}{\omega_p}\right)^{2n}}} = \frac{1}{\sqrt{1+\varepsilon^2\left(\frac{2\pi f}{2\pi f_c}\right)^{2n}}} \tag{2.4}$$

where n represents the filter order, fc the cut-off frequency, f the frequency and ε is the maximum pass band gain.

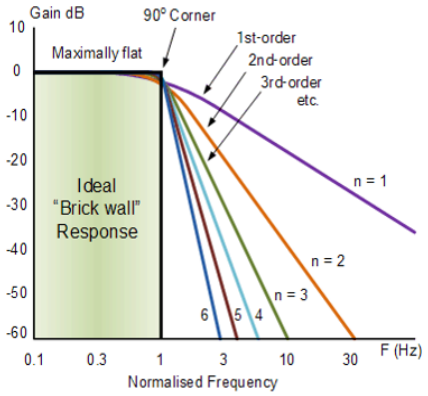

Figure 2.7: Frequency response of Butterworth filter in different order (Basic Electronics Tutorials, 2015).

2.8 Force platforms

Force platforms are structures that provide biomechanical data relative to the interaction between subject and the ground. Ground reaction force is the force supplied by the ground, and is described as the reaction to the force applied by the foot on the ground (Cavanagh and Lafortune, 1980).

These structures are composed by four tri-axial piezoelectric sensors, in which, the measured changes in pressures and forces are converted in electric voltage. The tri-axial axis corresponds to: transverse(X), anteroposterior(Y) and vertical plane (Z). Every single force (F) measure in the force plate is a result of the sum of the forces on the four sensors (Singhal et al., 2015). This method is represented in figure 2.8. It also should be noted the free moment (Tz) represented in the vertical component. This moment corresponds to coupling effects of the forces around de Z axis (Singhal et al., 2015).

Other important information that could be extracted from force platforms is the centre pressure. This corresponds to the point of application of the ground reaction forces on the plate (Cavanagh and Lafortune, 1980).

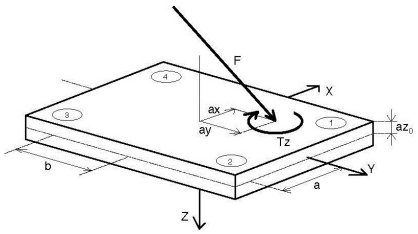

Figure 2.8: Force platform architecture and force diagrammed force vector (C-Motion, 2015).

2.9 Motion capture system

Motion capture systems are widely used in biomechanics studies to capture human movements (Reinbolt et al., 2011; Kar and Quesada, 2012; Steele et al., 2012; DeMers et al., 2014). Generally, motion capture techniques employs optical methods composed by a set of markers attached on the subject (Kirk et al., 2005). An array of cameras disposed around the laboratory observe and process the motion performed by the markers. A triangulation method is used based on the projection of the marker onto each camera plane. This method allows the time-varying location in space of each marker (Kirk et al., 2005).

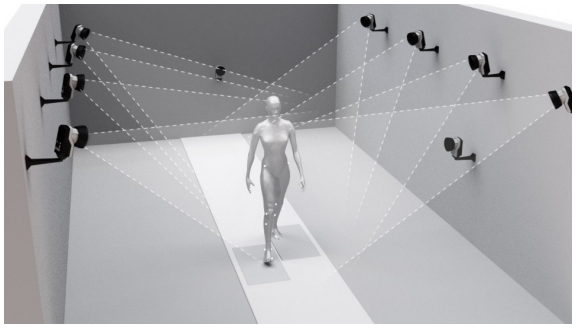

Figure 2.9: Optical motion tracker example architecture.

Important considerations when using this kind of system should be defined. First, has to be created a model that match the subject physical properties (Schönauer et al., 2011). Then, in order to determinate the subject movements, it is essential this model match the marker positions (Schönauer et al., 2011).

Once the signal is acquired it is crucial to process this data, in order to extract kinematic parameters, such as angles calculation. This step is necessary because the recorded data correspond only to the individual marker motion.

Consequently, it is necessary to define a marker labelling to identify each marker in its anatomical reference (Kurihara et al., 2002; Schönauer et al., 2011). After that, the model is defined by the connection of the markers in such way that replicates the human model. This increases the perception of the motion data, and then allows the calculation of body joint angles (Kurihara et al., 2002). Further information about this subject are explained in the following chapter.

2.10 Simulation

2.10.1 Musculotendon model

An important goal of this thesis is to understand the muscular behaviour during sport tasks, and how muscle react to an injury scenario. Hill-type musculotendon actuators are widely used in muscle-driven simulations (Zajac, 1989; Thelen, 2003; Millard et al., 2013). These actuators represents the musculotendon dynamics of human body muscle-driven simulations. Simplifications

relative to muscle architecture should be considered relative to musculotendon models. Muscle fibres geometry are assumed to be straight, parallel, coplanar and of equal length (Zajac, 1989; Millard et al., 2013). Musculotendon actuators consists in extensible strings tat wrap, and attach around biological structures as bones and tissues (Millard et al., 2013).

Hill-type muscle model is characterised by four characteristic curves that are represented in the following figure (Zajac, 1989; Thelen, 2003; Millard et al., 2013). In figure 2.10a) it is represented the musculotendon actuators phases which comprise an active contractile element, a passive elastic element, and at least, an elastic tendon (Millard et al., 2013). Moreover, it is important to distinct the dynamics of muscle tissues. Activation dynamics consists in the transformation of the neural excitation, provided by the nervous system, to activation of the contractile apparatus (Zajac, 1989). Muscle contraction relies on the transformation of activation on muscle force (Zajac, 1989).

Active force length curve $f^M(l^M)$ represents the force that a muscle is capable of f_0^M, relative to their nonlinearly length l_0^M (Millard et al., 2013). This force is generated by an active tension when the nervous system excites the muscles.

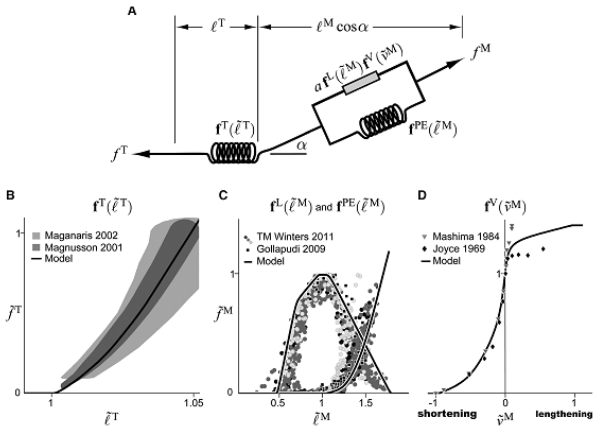

Figure 2.10: a) Hill-type model used to describe musclotendon dynamics. The model consists of a muscle contractile element in series and parallel with elastic elements (Thelen, 2003). b) tendon force-length curve; c) active and passive-force-length curves; d) force-velocity curve. These curves were normalized by the peaking at a force of f_0^M (Millard et al., 2013).

Passive-force-length $f^{PE}(l^M)$ consists in the force generated by the muscle that was stretched by a certain threshold of length, but is not fully activated. Muscle forces varies non-linearly with its rate of lengthening during non-isometric contractions (Millard et al., 2013). This behaviour is represented by the force-velocity curve $f^V(l^M)$.

Tendons are responsible to attach the muscles to the bones. These structures has elastic behaviour under tension, once they could stretch beyond its slack length l_s^T. By this way, tendons are modelled through a tendon-force-length curve $f^T(l^T)$ that represents the force developing by a non-linear elastic element (Zajac, 1989; Millard et al., 2013).

Applying these previous curves it is possible to compute muscle force (Millard et al., 2013):

$$f^M = f_0^M(af^L(l^M)f^V(v^M) + f^{PE}(l^M) \tag{2.5}$$

where a is the muscle activation. Muscle activation dynamics relies in a relation between muscle excitation (u) and muscle activation through a non-linear first order differential equation (Thelen, 2003):

$$\frac{da}{dt} = \frac{u-a}{\tau_a(a,u)} \tag{2.6}$$

where $\tau_a(a,u)$ is a time constant that varies according to activation levels (Thelen, 2003):

$$\tau_a(a,u) = \begin{cases} \tau_a(0.5+1.5a); & u > a \\ \tau_{deact}/(0.5+1.5a); & u \leq a \end{cases} \tag{2.7}$$

where τ_a is the activation time constant and τ_deact is the deactivation time constant. This relation concludes that the activation slows as activation level increases, once the levels of calcium provided by the sarcoplasmic reticulum to the muscle fibres are less efficient (Zajac, 1989; Thelen, 2003). Similarly, deactivation slows when muscle activation decreases due the fact the sarcoplasmic reticulum has less calcium ions to collect (Thelen, 2003).

2.10.2 Musculoskeletal model

In order to analyse knee joint injuries, it was necessary to use and develop a musculoskeletal model that best match and characterize human properties. An OpenSim model represents the dynamics of a system of rigid bodies and joints that are acted upon by forces to produce motion (Delp et al., 1990, 2007; Millard et al., 2013; Hicks et al., 2015). In this way, it was used a generic OpenSim model (Gait2392) as starting point to reach the goals of this thesis 2.11.

The Gait2392 model features 92 musculotendon actuators to represent 76 muscles in the lower extremities and torso. Moreover, this model includes three-dimensional, 23-degree-of-freedom joints of the human musculoskeletal system. Information relative to muscle parameters and inertial properties were described in Appendix.A. Once this model does not have patella, knee ligaments and patellar tendon, it was necessary to develop this human structures. Patella modulation and knee ligaments are explained in the following chapter.

2.10.3 Scaling

A major importance of simulation is ensure that a model is consistent with the human that was analysed. Scaling tool has the ability of scale the model to represent the experimentally measured size of the subject (Delp et al., 2007; Reinbolt et al., 2011). This procedure is based on relative distances between pairs of markers obtained from a motion capture system and the corresponding virtual marker location in the model (Delp et al., 2007). Moreover, this tool adjusts both the mass properties (mass and inertia tensor), as well as, the dimensions of the body segments (Delp et al.,

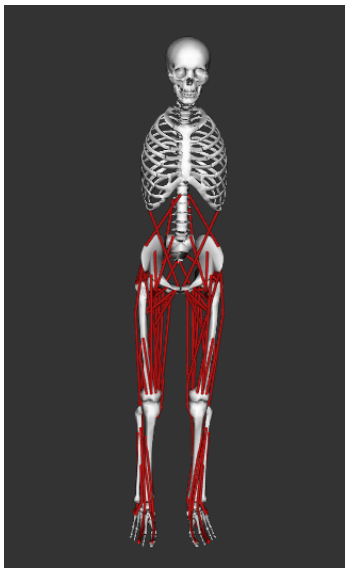

Figure 2.11: Musculoskeletal model Gait2392 (Delp et al., 1990).

2007; Reinbolt et al., 2011). Muscle properties as tendon slack length and fibre lengths, are also scaled in order to remain with the same percentage of total actuator length (Delp et al., 2007). Manual scale factors also could be applied to the model. This approach is based in anthropometric analysis.

Scaling is one of the most important steps in solving inverse kinematics and inverse dynamics problems because these solutions are sensitive to the accuracy of the scaling step (Delp et al., 2007; Shull et al., 2014). Generally, a static position is adopted to record the experimental marker position.

2.10.4 Inverse Kinematics

Inverse kinematics quantifies a set of joint angles and positions for the model that closely match the experimentally measured kinematics of the subject. Every time frame of an experimental trial is analysed, and according to this analysis, generalized coordinate values (angles and positions) are computed to a pose that match the experimental kinematics (Delp et al., 2007). This "match" is the pose that minimizes a sum of weighted squared errors of markers and/or coordinates (Delp et al., 2007; Reinbolt et al., 2011). After this step it is possible to see the motion that was matched in the user interface. It should be noted that this kind of evaluation only relies in kinematics. Muscle information is not processed is this tool.

2.10.5 Residual Reduction algorithm

Generally, modelling and marker processing data are associated to some errors, which in a certain point, aggregate and lead to non-physical compensatory forces known as residuals (Anderson and Pandy, 1999; Kar and Quesada, 2013; Hicks et al., 2015). Residual reduction algorithm is a

process of optimization relative to joint forces calculation and kinematic biases (Delp et al., 2007; Kar and Quesada, 2013).

From Newton's second law, the following equation relates the measured ground reaction force and gravitational acceleration to the accelerations of the body segment (Delp et al., 2007):

$$\vec{F}_{external} = \sum_{i=1}^{segments} \vec{m}_i \vec{a}_i - \vec{F}_{residuals} \tag{2.8}$$

$$\vec{F}_{residuals} = m_{additional} g_{acc} \tag{2.9}$$

where $\vec{F}_{external}$ corresponds to the ground reaction force, which is defined by the mass of each body segment, $\vec{m}_i$, and $\vec{a}_i$ its translational acceleration. $\vec{F}_{residuals}$ is defined by the additional mass due to residuals $m_{additional}$, and g_{acc} gravitational acceleration.

Based on equation 2.9, the residuals are associated to an additional mass that will be assumed in the segment mass calculation (Kar, 2011). The main advantage of this algorithm, is the ability of processing the kinematics of the model from Inverse Kinematics, in order to, be more dynamically consistent with the ground reaction force data (Hicks et al., 2015). For that, residuals are reduced by small adjustments to the mass parameters of the model, as well as, controlled perturbations to the motion trajectory (Delp et al., 2007). Changes at the location of the centre of mass of the torso, are recommended by this algorithm once contributes to the reduction of residuals during the movement (Delp et al., 2007).

2.10.6 Static Optimization

Muscle activations and forces during sports tasks are important information to understand how an injury scenario occurs. Most important is the ability to process this information, in order to, prevent this from happen. Static Optimization is a method that estimates muscle forces and activations that satisfy motion parameters as accelerations, positions, velocities and ground reaction forces (Anderson and Pandy, 2001). Indeed, it is an inverse dynamics approach. This method is defined as "static" once estimations are performed without integration of equations of motion between time steps. As these estimations are performed only at each time frame, Static Optimization can be very fast and efficient. However ignores activation dynamics and tendon compliance (Lin et al., 2011)

Based on musculoskeletal geometry assumptions about force distribution to estimate individual muscle forces are evaluated. However, this technique relies in a muscle force distribution problem. Since the musculoskeletal system is mathematically a redundant force system, as consequence, has more unknown forces that equilibrium equations (Heintz, 2006). In this context, optimization methods based on performance criterions are widely used to solve this problem (Anderson and Pandy, 2001; Heintz, 2006; Hewett et al., 2005b).

The muscle activation-to force conditions output from Static Optimization were defined based on the following equations (Anderson and Pandy, 2001):

where a_m is the activation level of the muscle **m**, at a discrete time instant defined by (t_i). Each muscle was assumed to be an ideal force generator:

$$F_m(t_i) = a_m(t_i)F_m^0 \tag{2.10}$$

where $F_m(t_i)$ is the force generated by the m muscle and correspond to its maximum isometric force. In contrast, force generator could be constrained by force-length-velocity properties:

$$F_m(t_i) = a_m(t_i)f(F_m^0, l_m, v_m) \tag{2.11}$$

where $f(F_m^0, l_m, v_m)$ correspond to the force-length-velocity assumed in the musculoskeletal model, and the shortening velocity and the length of muscle m (Zajac, 1989).

The performance criterion relies on minimizing the activation squared summed across all the muscles (Anderson and Pandy, 2001):

$$J_i = \sum_{m=1}^{musculotendon-actuators} (a_m(t_i))^2, i = 1, .., n_{segments} \tag{2.12}$$

Other methodology used in Static Optimization, as a performance criterion, is minimize the muscle stress, once activation level could be described such as (Anderson and Pandy, 2001; Hicks et al., 2015):

$$a_m = \frac{F_m}{F_m^0} = k\frac{F_m}{PCSA} \tag{2.13}$$

$$J_i = \sum_{m=1}^{musculotendona-actuators} \left(k\frac{F_m}{PCSA}\right)^2 \approx \sum_{m=1}^{musculotendon-actuators} (a_m(t_i))^2, i = 1, .., n_{segments} \tag{2.14}$$

where k is a user defined constant.

2.10.7 Analyse tool

The major goal of a simulation is the ability of answering to specific research questions. By this way, Analyse Tool (figure 2.12) included in OpenSim, allows to analyse a model or simulation based on a number of inputs that were performed in different phases of simulation. The major advantage of this tool is that require low computational time. As consequence, has the ability of quickly process kinematic, kinetic and muscle data in order to provide contents relative:

1. **Muscle analysis**: Reports all attributes of all muscles (including fibre length and velocity, normalized fibre length, pennation angle, active-fibre force, passive-fibre force, tendon force, and more).

2. **Joint reactions**: Calculation of resultant forces and moments at joints.

3. **Actuation**: Records the generalized power, speed and force developed by each actuator of the model.

4. **Kinematics**: Generalized coordinates, speeds and accelerations.

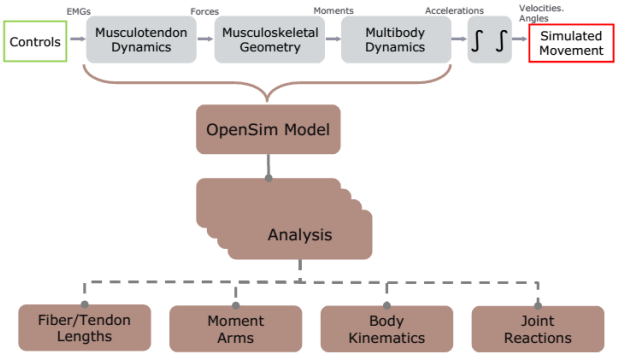

Figure 2.12: Analyse tool inputs and outputs data (Groote et al., 2016).

2.10.8 Joint reaction

Joint Reaction it is an OpenSim analysis tool which calculates resultant moments and forces at the body joints (Steele et al., 2012; DeMers et al., 2014). This method is applied between two contacting bodies as a result of all the forces acting on the model. These forces and moments represents the internal load, in which joints structures are subjected at a certain motion (Steele et al., 2012; DeMers et al., 2014). For instance, this approach reports the sum of contact forces between femur and patella.

In order to, perform this analysis it is essential to solve generalized equations of motion (Steele et al., 2012). These equations are related to generalized coordinates and generalized forces of the model. For that, Joint Reaction uses the output files of Static Optimization and RRA, kinematics and muscle forces respectively. Therefore, a post processing procedure is used to calculate resultant joint loads (Steele et al., 2012; DeMers et al., 2014):

$$\vec{R}_{knee} = [M]_{tibia}\vec{a}_{tibia} - (\vec{R}_{ankle} + \sum \vec{F}_{muscles} + \vec{F}_{gravity}) \tag{2.15}$$

where $\vec{R}_{knee}$ is the force from the femur on the tibia, $[M]_{tibia}$ is the matrix of inertial properties of the tibia, $\vec{a}_{tibia}$ is the six dimensional angular and linear acceleration of the tibia, $\vec{R}_{ankle}$ is the force from the foot on the tibia, and $\vec{F}_{gravity}$ and $\vec{F}_{muscles}$ are the gravitational and muscle forces acting on the tibia.

In figure 2.13 is described the joint centre of both parent and child bodies, in which reaction loads acts. In Joint Reaction editor is possible to define a specific or all the joint of the model. Furthermore, the correspondent child and parent frames relative to the reported forces also could be defined.

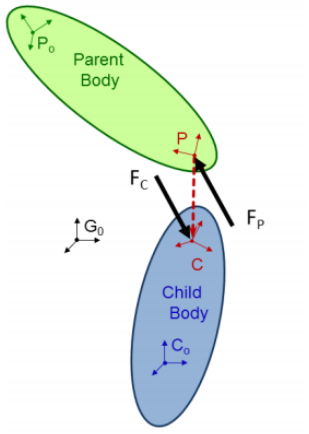

Figure 2.13: Joint load representation (DeMers et al., 2014). G_0 origin of the ground reference frame; P_0 origin of the parent body and reference frame; C_0 origin of the child body and reference frame; P: location of the joint in the parent body; C: location of the joint in the child body; F_p Joint reaction load on the parent body; F_c Joint reaction load on the child body.

Chapter 3

Materials and methods

Acquire motion data is complex and involves multiple steps that are co dependent of each other. It is essential to project the experimental protocol, in order to optimize the trials duration in a efficient way. A workflow showing the sequence of events is given in figure 3.1. Subjects performed drop jumps from different heights ranging from 30-60 cm in steps of 15 cm. The changes in height serve as variable to increase the task difficulty and possible loading on knee joint.

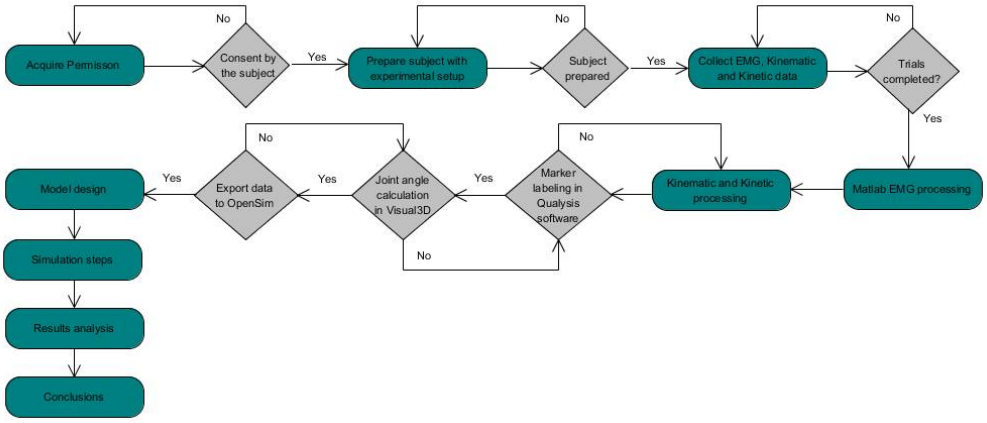

Figure 3.1: Project workflow

This section focus on experimental setup, steps and procedures to prepare the subject, data acquisition, and at least details for data processing and data analysis.

The applied methodology consists in the processing phase, in which all the inputs relative to the experimental data, musculoskeletal and musculotendon properties were defined. Therefore, is possible to extract the experimental EMG activation data that will be used in the simulation validation. Moreover, through the model design, the joint angles and GRF will be possible to perform the different steps of the musculoskeletal simulation. Figure 3.2 illustrates all the steps applied in this methodology.

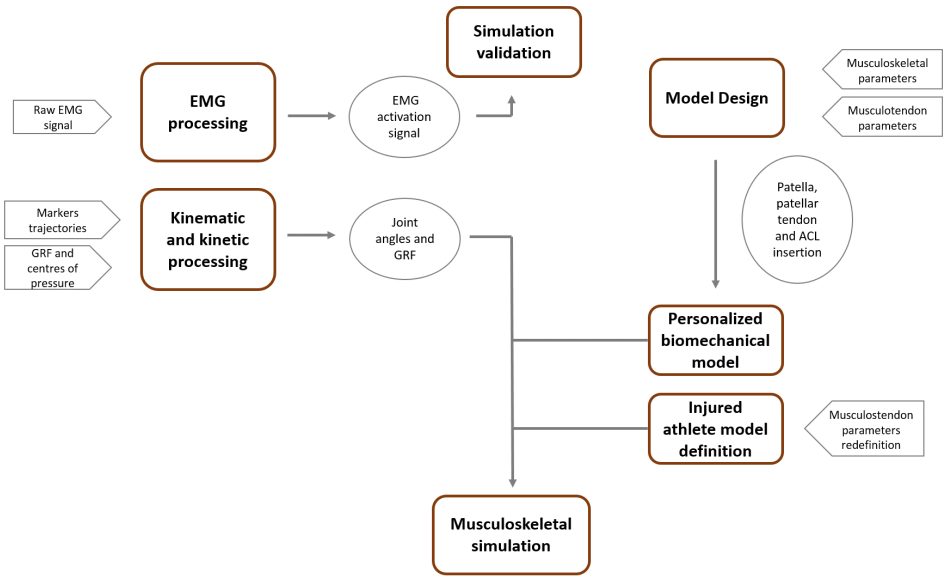

Figure 3.2: Methodology steps.

3.1 Experimental setup

Drop jumps tasks were performed by one volleyball female athlete (female, age 22, mass 73 kg, height 1.80 m), in order to collect kinematic and kinetic data as input from OpenSim software. Moreover, EMG signals were also collected. This athlete was informed before the beginning of the trials relative to the desired tasks and its risks.

Kinematic data was acquired with 12 Qualisys infrared retroflective cameras (Qualisys AB, Sweden) at a sampling frequency of 200 Hz. The motion capture markers were attached according to a full-body marker set reported by (Jan, 2007). Kinetic data was collected by four force platforms (Bertec, Columbus, USA) at 2000 Hz. EMG acquired with 10 wireless Trigno sensor (Delsys Inc. Boston, MA, USA) at a sampling frequency of 2000 Hz. The EMG and force data was synchronized with the motion capture by mean of an Analog-to-Digital converter. By this way, temporal alignment was ensured to all equipments during the trials. A set of gym steps were also used to increase the drop jump height.

3.2 Preparing the subject

In the beginning, it was explained the goals of the thesis to the female athlete, in order to her understand what kind of task she should perform. Moreover, it was explained that eventual minimal injury risk could be present on these trials. Then, the female athlete signed a consent form stating their intention to participate on the trials.

Anatomical measurements were then acquired relative to height, body mass and segments anthropometry. Forty three marker and four clusters were positioned at specific anatomical reference

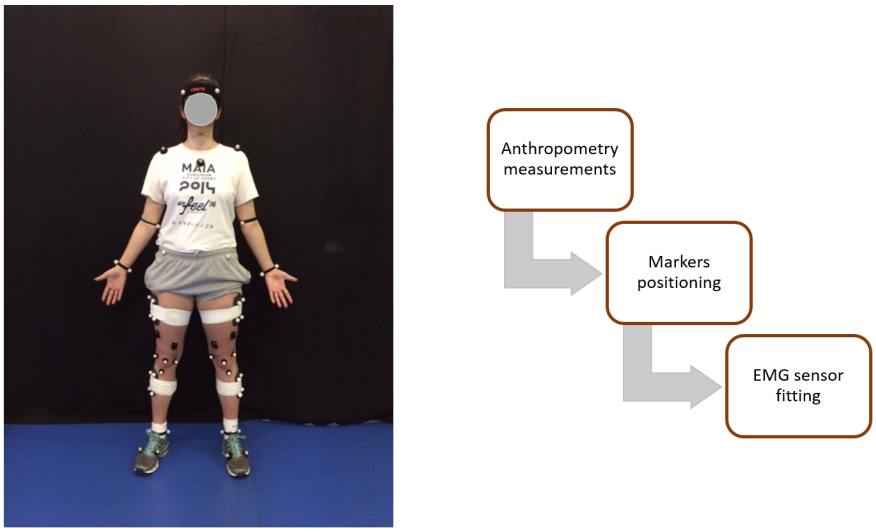

Figure 3.3: Subject preparation.

points (figure 3.3). The clusters were attached on the shank and thigh of both legs. Moreover, the subject was fitted with 10 EMG sensors relative to the left and right rectus femoris, quadriceps, hamstrings and gastrocnemius muscles.

3.3 Trial procedure

These trials were made to evaluate the drop jump movement and their risk to knee joint integrity. For that, it was collected three drop jumps from different heights, in order to increase knee joint injury risk. The heights were 30, 45 and 60 cm.

The different phases of these trials are illustrated in figure 3.4. In the first phase it was necessary to calibrate the virtual space, in which the trials will be performed. While this task was done, the subject performed a warm up which consists in 5 minutes running on the laboratory treadmill. Then, it was necessary to collect static motion with erect posture, to scale body segments and align joints (Kar and Quesada, 2013). Static trials were recorded during five seconds. Then the subject was instructed to perform a drop jump by standing on a gym step, and jump to the force plates with one foot in each platform. Every jump was repeated three times at each height, in order to collect the most precise and accurate data.

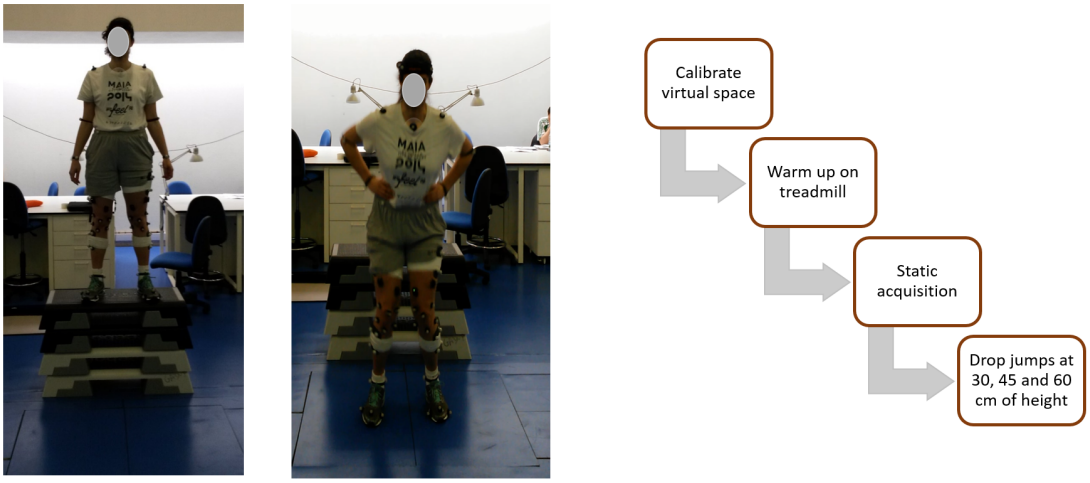

Figure 3.4: Drop jump trial procedure.

3.4 EMG data processing

EMG activity from quadriceps and hamstring were processed, from both legs. Generally, EMG processing in simulation works has a common processing pipeline (Delp et al., 1990; Hamner et al., 2010; Steele et al., 2012; Gerus et al., 2013; DeMers et al., 2014). First, the raw signal were band pass filtered (20-1000 Hz), full wave rectified, low pass filtered through a Butterworth filter(4th order, 40 Hz cut-off frequency), and at least normalized by the maximal isometric contractions obtained during the trials. Moreover, it was used a RMS approach to convert the normalized EMG signal in an amplitude envelope.

The bandwidth was (20-1000 Hz) in order to remove electrical noise and biological artefacts that contaminate the raw signal. The final EMG signal consists in an amplitude envelope that varies between 0(fully deactivated) and 1(fully activated) (Hamner et al., 2010). This approach identifies the rapid changes in the muscle activity during such contraction by using short duration sampling windows. Matlab software was used to perform the applied processing pipeline. In the figure 3.5, it is described the position of Trignos modules over the analysed muscles.

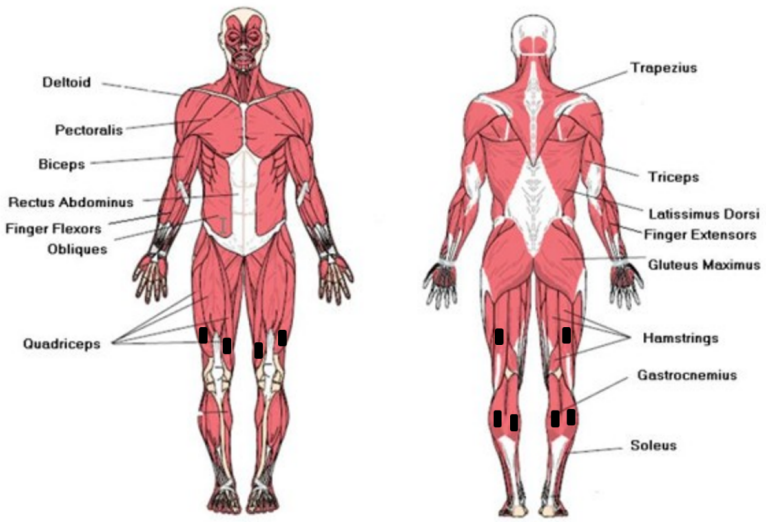

Figure 3.5: Trignos position on subject quadriceps, hamstrings and gastrocnemius.

3.5 Kinematic and kinetic data processing

Processing kinematic data was an important step of this work. As mentioned in the previous chapter, motion data recorded by the markers and Qualysis systems only relies on the individual markers motion (figure 3.6). First part of this processing was relative to marker labelling according to its anatomical position. It was selected every marker and gap filled parts were deleted. This procedure is very important to the software does not assume wrong marker position.

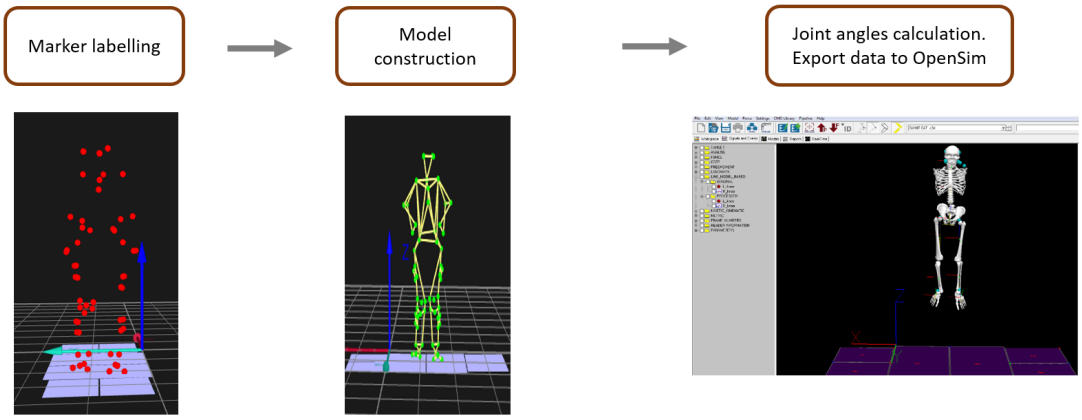

Figure 3.6: Kinematic and kinetic processing steps

Next, it was necessary to create a model on Qualysis software. This model allows the calculation of angles between joints, and is important to process the marker behaviour during the

trial because increases the visual aspect. Moreover, with the model creation time dispensing was reduced in the next data trials, once the model by himself will identify the marker label. Therefore, through a polynomial interpolation method it was analysed the graph fill trajectory of every marker in order to fill some gaps. By this way it is possible to increase the accuracy of kinematic data.

OpenSim software needs as input two files with the kinematic and kinetic trail histories respectively. For that, it was necessary assure the compatibility of the experimental data with OpenSim. Once this does not read c3D files it was used a software capable to export the c3D files to Opensim. For this purpose Visual 3D was used. Visual3D exports an OpenSim compatible motion file, which bypasses the Scaling and Inverse Kinematics (IK) in OpenSim and can be used directly by the OpenSim Residual Reduction Algorithm. For that, computed scale factors will scale the OpenSim gait model from the Visual3d static calibration model.

3.6 Model design

In order to perform simulations at the knee level according with our thesis goals, it was necessary to use a musculoskeletal model that best reproduces knee biological structures. It was used a generic OpenSim model Gait 2392 (Delp et al., 1990) as starting point. Once this model does not includes ACL ligaments, patella and patellar tendon, it was necessary to modulate this structures on the Gait 2392 model. The resultant model is illustrated in the following figure 3.7:

Model degrees of freedom (DOF) included a ball-and-socket joint connecting the pelvis to the torso, three rotations and three translations of the pelvis, a ball of socket joint at each hip, and revolute ankle and subtalar joints (Lerner et al., 2015).

Knee joint was defined has 3 rotational and 2 translational DOFs at the sagittal plane (figure 3.8). The rotations includes flexion/extension movements going through the knee joint centre and perpendicular to the plane. Internal/external rotations were defined as a hinge joint with its axis going through the ankle joint and knee joint centres. At least, abduction/adduction movements were defined by two hinge joints, with the axes perpendicular to the tibial frontal plane going through medial and lateral condyle contact point. The two translational DOFs were defined as the anterior-posterior and superior-inferior translations of the tibia as a function of knee flexion angle (Gerus et al., 2013). This movement englobes the translation of the knee joint centre relative to the origin of the femoral head (Gerus et al., 2013).

The model was driven by 92 muscle-tendon actuators, with muscle geometry and architecture based on the model of (Delp et al., 1990). Once this study was based on female athletes a scale factor of 0.75 were used to match its muscle properties according to (Thelen, 2003). Optimal fibre length and tendon slack length were the same of (Delp et al., 1990). The reason was that female-to-male height ratio was similar (Thelen, 2003). Every information about the model is described precisely on the appendix A.

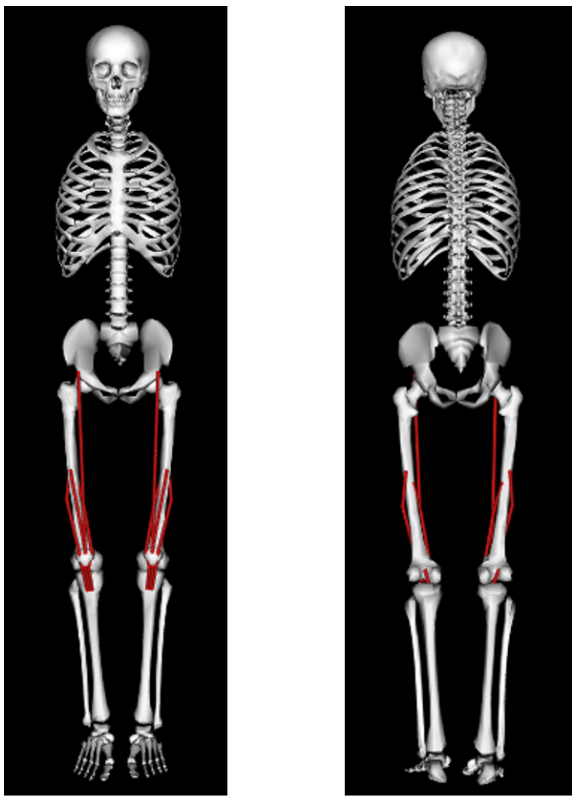

Figure 3.7: a) Anterior view b) Posterior view.

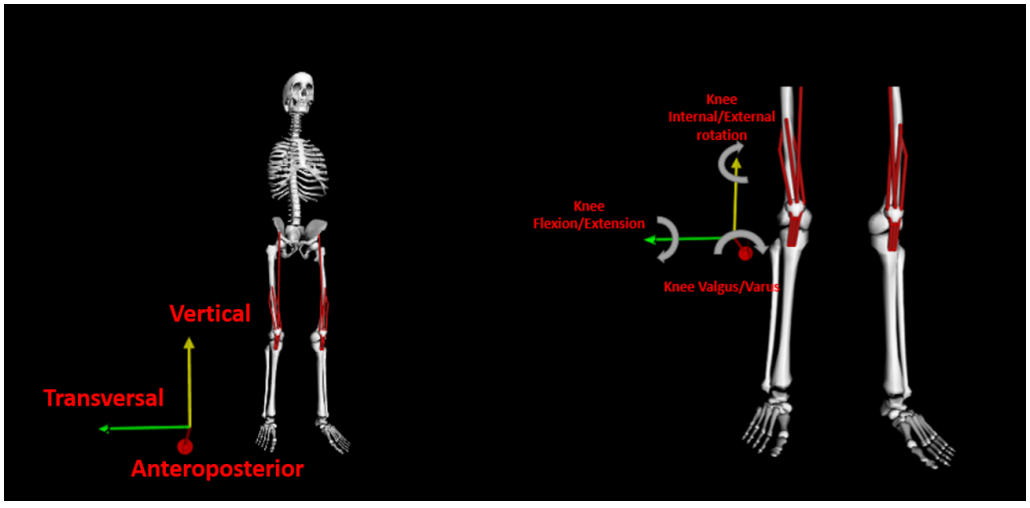

Figure 3.8: Model axis and knee defined DOFs.

Furthermore, to test and understand the behaviour of an injury athlete on drop jumps, it was changed some muscle parameters. For that, it was assumed muscle parameters of an old subject used in the work of (Thelen, 2003). In addition, optimal fibre length was also changed. The defined muscle parameters for the injury athlete are represented in the following table 3.1: where

Table 3.1: Muscle parameters for injured model.

	τ_{deact}	$V^M_{\max}$	ε^M_0	$\vec{F}^M_{len}$	L^M_0	F^M_0
Healthy	50	10	0.6	1.4	-	-
Injured	60	8	0.5	1.8	-25%	-30%

τ_{deact} is the deactivation time constant, $V^M_{\max}$ the maximum muscle contraction velocity expressed in optimal fibre lengths (L^M_0), ε^M_0 the passive muscle strain due to maximum isometric force, $\vec{F}^M_{len}$ the ratio of maximum lengthening muscle force to isometric force, L^M_0 the optimal fibre length, and at least F^M_0 the muscle maximum isometric force.

Muscle forces were also reduced 30% from values used in female young athletes. This assumption is based on studies that relate the occurrence of knee injuries relative to low capacity of force generation from some muscles. Quadriceps weakness are the most common scenario in knee injuries as patellofemoral maltracking and patellofemoral pain Mason et al. (2008); Fulkenson (2004).

Other important parameter change was relative to optimal fibre length. This property is defined as the muscle length in which muscles generate maximum force. In injury athletes optimal fibre length is shorter than healthy athletes, once the muscle generate force at shorter muscle length. This is characterised as a risk factor for some research authors (Liu et al., 2012).

These muscle properties were assumed to characterize an injury athlete. In this way, it is possible to compare healthy and injured athletes in drop jumps and collect important muscle, kinetic and kinematic data. These muscular changes were only applied on quadriceps muscle and ACL ligament.

3.6.1 ACL modelling

ACL modelling represented on figure 3.9 was based on the work of (Kar and Quesada, 2012) available on Simtk.org web page. ACL was defined as a passive soft tissue with only one fibre bundle, once anteromedial (AM) and posterolateral (PL) bundles, were assumed to have similar characteristics. The insertion point on the body segments were defined on the femur and tibia. The superior part was attached into the depths of the inter-condyloid part of the femur while the lower part on the front meniscules of tibia (Kar and Quesada, 2012). It was necessary to scale this tissue to our subject anthropometry.

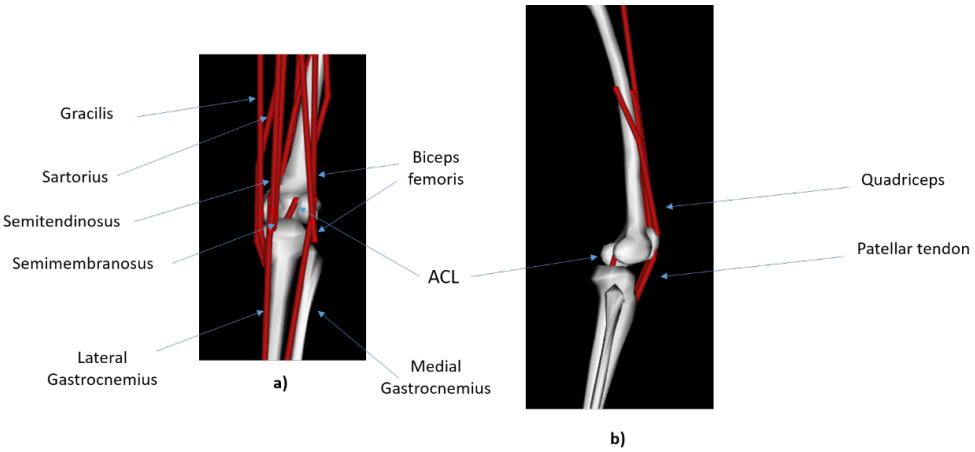

Figure 3.9: ACL modelling:a) Posterior view; b) Lateral view.

3.6.2 Patella and patellar tendon modelling

Patella insertion on the gait 2392 had required a redefinition of the knee mechanism. Initially, without the presence of the patella, insertions of the quadriceps were handled with moving points in the tibia frame. In this work, the patella segment (figure 3.10) was articulated with the femoral-condyle (Seeley et al., 2005). The quadriceps wrapped at the top part of patella (DeMers et al., 2014; Lerner et al., 2015), and the patellar tendon attach the lower part on the tibial tuberosity (Xu et al., 2015). This configuration allows the redirection of quadriceps forces to act along the line of action of the patellar tendon (DeMers et al., 2014; Lerner et al., 2015). The patellofemoral and tibiofemoral joints were modelled with rotations and translations constrained to the knee flexion angle.

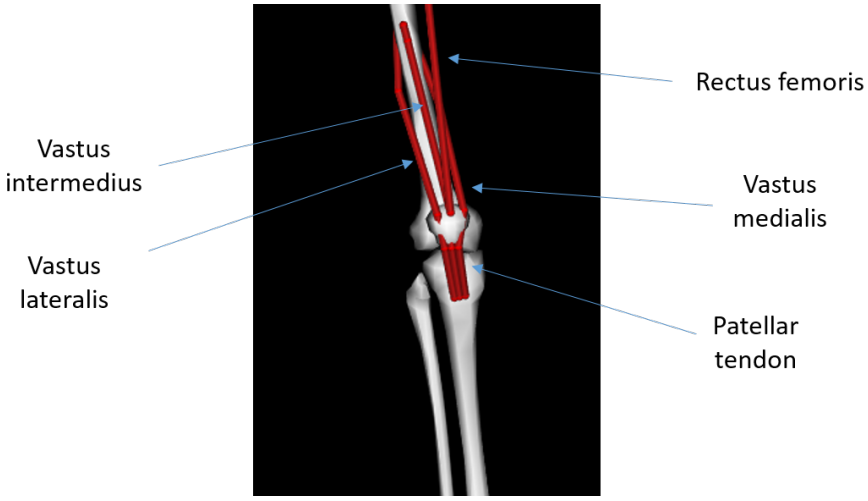

Figure 3.10: Patella and patellar tendon modelling.

3.7 Musculoskeletal simulation

Figure 3.11 illustrates the simulations steps that were performed to simulate the drop jump movement. First, Scaling step computes scale factors that will scale the Opensim model to match the anatomical properties of the subject. Once kinematic and kinetic data processing are associated to some errors, it is crucial to reduce the residuals that were created. Adjustments on the torso mass and kinematic filtering were applied through RRA step in order to eliminate this residuals forces. At this point internal muscle forces and activations were not generated. Static Optimization will compute these two properties, in order to provide the input files for Analyse tool.

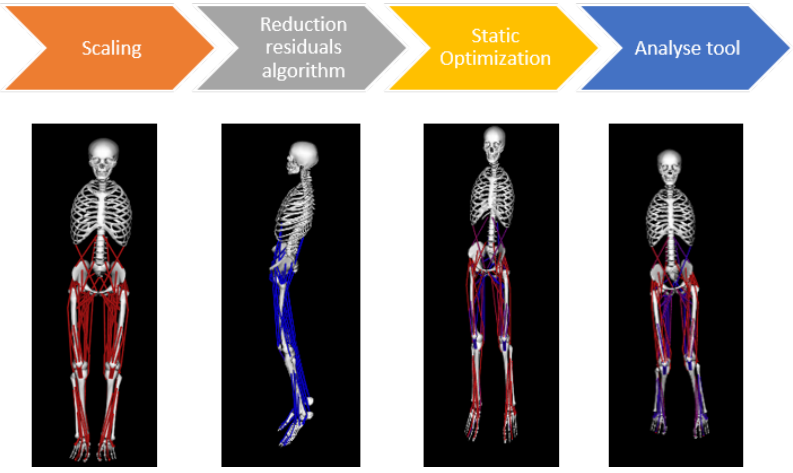

Figure 3.11: Dynamic simulation workflow.

3.8 Drop jump

Drop jump is a common movement to analyse human motion tasks because allows to extract important information relative to injuries scenarios (Kar, 2011; Dowling et al., 2012; Nyman and Armstrong, 2015). In volleyball movements, this movement could be seen in two particular situations: landing from an attacking move and landing from a successful or unsuccessful block (Zahradnik et al., 2014).

In figure 3.12 could be seen the different phases of drop jump and the forces applied by the ground on the force plates. The starting phase is relative to an upright position with the hands

parallel to the torso. Then an eccentric phase begins when the subject reaches the ground flexing the knees and hips. Following, a concentring phase is characterised by the extension of the knees and hips with the hands on the waist to jump vertically as high as possible. A minimum stop between the eccentric and the concentric phases could be verified, which is the result of the energy stored by the elastic elements of the muscles (Ortega et al., 2010).

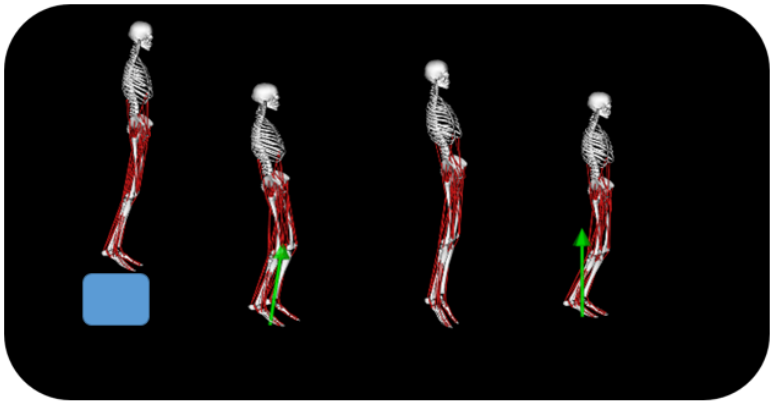

Figure 3.12: Drop jump phases and force plates contact forces.

One of the important phases of this jump is the landing phase (Ferretti et al., 1992; Zahradnik et al., 2014). The typical landing follows a toe-heel pattern, which is characterised by two peaks. The first corresponds to the initial contact to the ground, and the second one, to the moment when the heel contacts the ground during the toe-heel landing after the forefoot (Ortega et al., 2010; Zahradnik et al., 2014).

3.9 Simulation validation

Evaluation the accuracy and credibility of modelling studies is essential to assure the correct assumption between the models and the reality. Modelling the neuromusculoskeletal system and its corresponding motion is a delicate and complex task. This involves methods to represent multi-body dynamics, contact forces, musculo-tendon dynamics, musculoskeletal geometry and neural control (Hicks et al., 2015).

In this work every result of the simulation steps were analyse based on the good practices of validation reported by (Hicks et al., 2015), and disposable online in www.simtk.org. Kinematic data were compared between the experimental inverse kinematics and the simulation step RRA. Muscle activations were compared to experimental EMG in order to evaluate if the two signals have some similarity.

In addition, it was used Pearson correlation to analyse the relationship between experimental and simulated data. This methodologies were applied on the data through MATLAB routines.

3.10 Simulation outputs for injury prevention

Based on the review of injury scenarios in the first chapter, a set of parameters were defined to test their behaviour on drop jumps simulation. Kinematic parameters were relative to hip adduction, knee flexion/extension, internal/external rotations and valgus/varus angles. ACL properties as fibre length and power were also analysed. These are important variables, once represent ACL loading during the time.

Muscle activations relative to hamstrings, quadriceps and gastrocnemius were also calculated. These activations are important to understand the ratios between hamstrings and quadriceps, and gastrocnemius and quadriceps, in order to evaluate muscle weakness. These ratios were calculated based on the following equation:

$$ratio = \frac{\sum mean_{flexors}}{\sum mean_{extensors}} \tag{3.1}$$

where $\sum mean_{flexors}$ is relative to the sum of the mean value of the flexors, in case of hamstrings the bicep femoris, and relative to medial and lateral gastrocnemius. $\sum mean_{extensors}$ is relative to the sum of the mean value of the extensors, relative to quadriceps, most concretely the vastus medialis and vastus lateralis.

Chapter 4

Results and discussion

In this chapter are presented all the results from the simulations that were performed. It was analysed in detail every kinematic, kinetic and muscular data, relative to drop jumps at different heights.

In addition, it was made a comparison between a healthy and an injured athlete, in order to understand how kinematic, kinetic and muscular patterns vary. More important this information could be suitable to understand how an injury occurs.

It was selected only the landing phase of drop jump, once is the phase where are more probability of an injury occur (Ferretti et al., 1992; Zahradnik et al., 2014). It is important to refer that the peaks represented in the following graphs are correspondent to the maximum value of the different parameters during the landing phase. This phase is relative to the initial contact with the ground until the preparation to the second jump (takeoff).

4.1 Simulation validation

Kinematic data were compared between the experimental inverse kinematics (IK) and the simulation step RRA. In the figure 4.1 is the result of the comparison in knee angle flexion. Pearson correlation calculations showed high accordance between the two steps. For the right knee flexion was 0.9981 and 0.9986 for right and left leg respectively. These values also mean that the residuals were low in the simulation.

Static optimization activation values were compared with the EMG experimental data in figure 4.2. Analysing the on/set and off/set of activation values it was possible to conclude that the values of the simulation show some accordance with the experimental EMG data. However, Static Optimization ignores activation dynamics represented in 2.7. Hence, electromechanical delay was not assured and some deviation between experimental and simulated results could be verified.

In addition, it was tested the accuracy of the force values generated by the simulation for the different muscles. Through the joint reaction, hip joint moments were calculated. As this joint is a ball-and-socket joint zero values for knee moments should be noted, once no forces could be produced to constrain the rotation of the femur (DeMers et al., 2014; Hicks et al., 2015). Indeed,

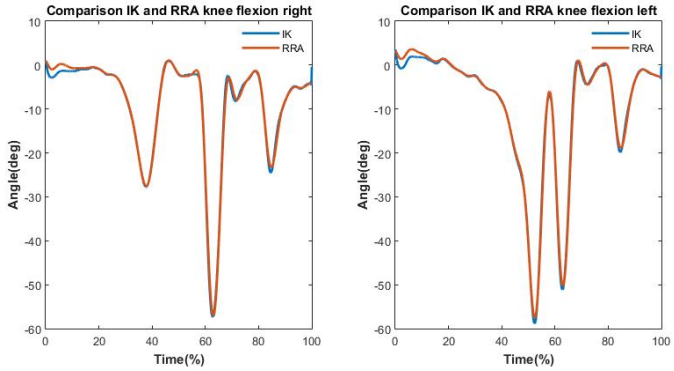

Figure 4.1: IK and RRA comparison.

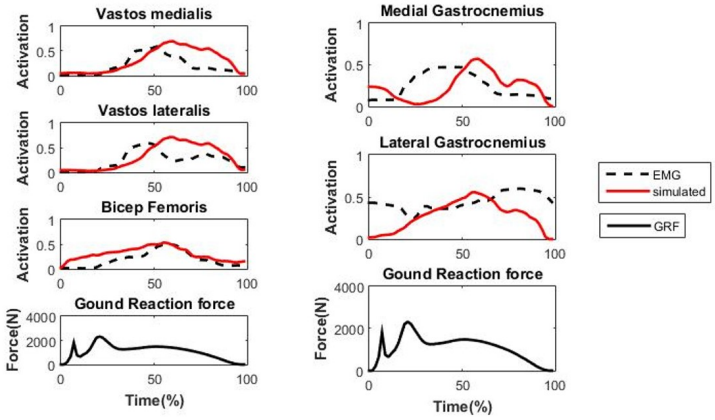

Figure 4.2: Comparison experimental EMG with simulated activations.

it was possible to prove this fact in our simulations and validate our results.

4.2 Drop jump trials: Height analysis

4.2.1 Kinematic data

4.2.1.1 Knee angle extension/flexion angles

Low knee flexion angle is considered a risk factor in landing tasks that are associated to ACL injury and patellar disorders. In figure 4.3 is described the knee flexion angle during the drop jump at different heights. The peak knee flexion at 30 cm for the right leg was 44.63 degrees and for left leg was 42.60 degrees. The peak knee flexion at 45 cm for the right leg was 58.12 degrees and left leg was 54.85 degrees. The peak knee flexion at 60 cm for the right leg was 57.25 degrees and left leg was 54.41 degrees.

Generally, ACL injuries occur when the knee flexion angle is less than 30 degrees (Dai et al., 2014; Zahradnik et al., 2014) about 40 ms after initial foot contact with the ground (Krosshaug

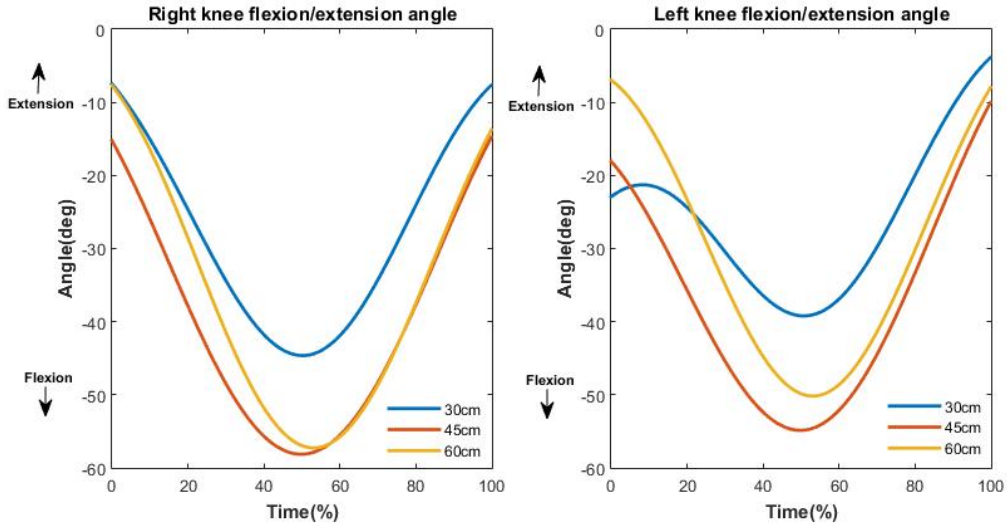

Figure 4.3: Knee flexion/extension angles at different heights.

et al., 2007). According to this data knee flexion angle was ever superior that 30 degrees. It could be concluded that independent of the height increasing, ACL integrity in these trials were not compromised. As higher are knee flexion angles, more energy is absorbed by the quadriceps which preserves the ACL tensile forces (Zahradnik et al., 2014; Nyman and Armstrong, 2015). It was noted that the peak values from 45 cm were higher that 60 cm trials. This phenomenon indicate that a threshold peak was reached for knee flexion angle (Kar, 2011). This effect was also verified in the work of (Peng et al., 2011). Obtained knee flexion angles showed some similarity with these works (Malfait et al., 2016) and (Bates et al., 2013).

4.2.1.2 Hip abduction/adduction angles

In figure 4.4 is describe the hip adduction angle during the drop jump at different heights. The peak hip adduction angle at 30 cm for the right leg was 8.40 degrees and for left leg was 0 degrees. The peak knee hip adduction angle at 45 cm for the right leg was 9.13 degrees and left leg was 0 degrees. The peak hip adduction angle at 60 cm for the right leg was 1.51 degrees and left leg was 0.30 degrees.

In right leg hip adduction angle was higher at 45 cm. A possible reason could be muscle hamstrings and quadriceps weakness (Powers, 2010). In the left leg it was verified a different scenario. The subject has a landing phase with more hip adbuction than hip adduction. This effect was verified in all different heights. Unfortunately, is not well understood in the literature the effect of hip abduction in knee injuries. Meanwhile, stronger hip abductors show less hip adduction (Souza and Powers, 2009; Ferber et al., 2011).

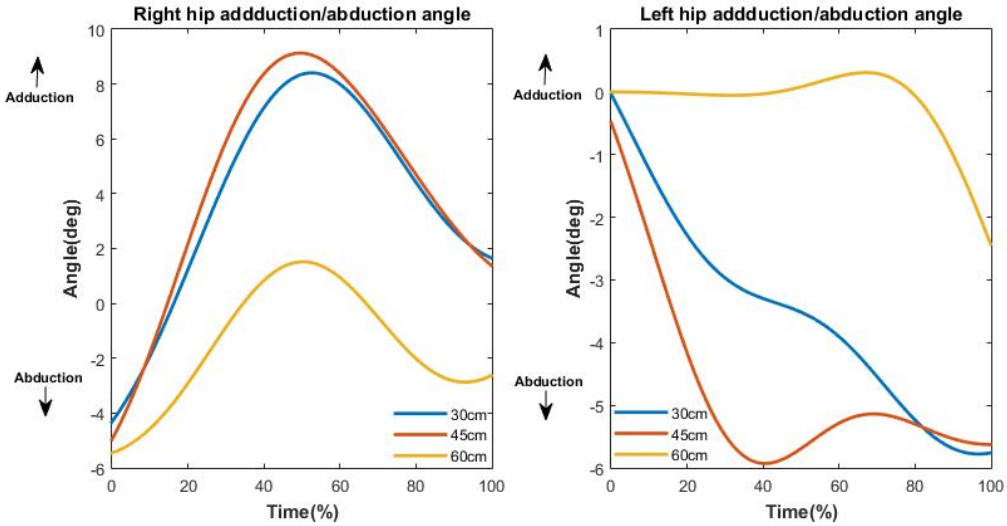

Figure 4.4: Hip abduction/adduction angles at different heights.

4.2.1.3 Knee valgus/varus angles

In figure 4.5 is describe the knee valgus angle during the drop jump at different heights. The peak knee valgus at 30 cm for the right leg was 2.62 and for left leg was 0.91 degrees. The peak knee valgus at 45 cm for the right leg was 1.13 degrees and for left leg was 0.11 degrees. The peak knee valgus at 60 cm for the right leg was 2.61 degrees and for left leg was 0.58 degrees.

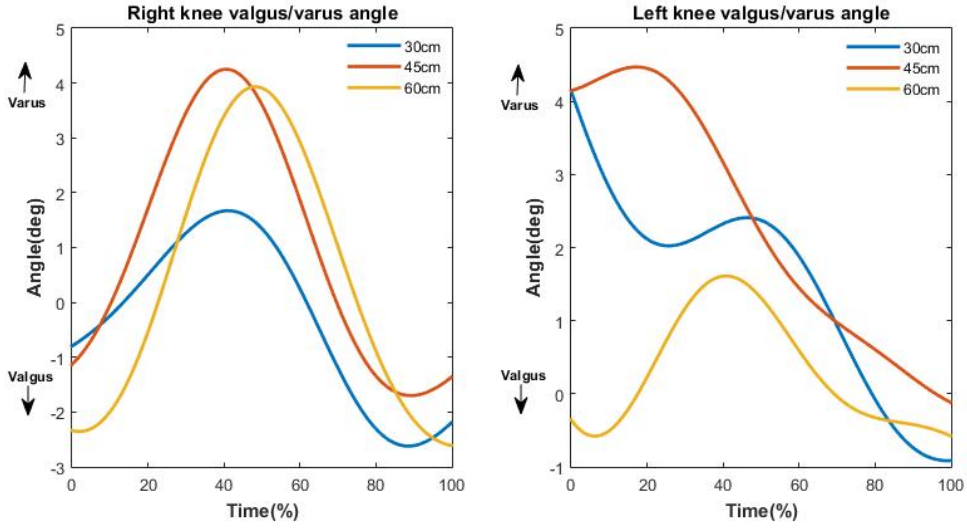

Figure 4.5: Knee valgus/varus angles at different heights.

It could be seen that knee valgus is greater at 60 cm in the right and at 30 cm in the left leg. Higher knee valgus was verified in right leg relative to left leg. In contrast left leg showed higher knee varus at the initial contact. An exception was the 60 cm trial that showed higher valgus in

the initial contact. However, following the maximum flexion phase the subject showed that knee valgus values were higher in both legs. A possible explanation for higher knee valgus in the right leg may be that, right leg reach the ground first relative to left leg. In this way, supports the body height in a first phase. In addition, higher hip adduction values were verified in figure 4.4 which implies higher valgus (Powers, 2010).

These results are in accordance with the work of (Hewett et al., 2005a), in which compared injured and uninjured athletes in a drop jump landing task at 30 cm. In this work, ACL rupture occurred at 9 degrees of knee valgus. In comparison, the results of knee valgus of our work were lower. Similar results were also verified with these works (Bates et al., 2013; Cruz et al., 2013; Kar and Quesada, 2012) relative to 30 and 45 cm heights . However, it was not seen that knee valgus is higher as height increases. It could be concluded that 60 cm trial was the most demanding trial. Indeed, higher knee valgus increase ACL strain and internal forces increasing the probability of the ACL rupture and patellar disorders occur (Kar and Quesada, 2012; Dai et al., 2014).

4.2.1.4 Knee external/ internal rotations angles

In figure 4.6 is describe the knee internal/external rotations during the drop jump at different heights. The peak knee external rotation at 30 cm for the right leg was 5.27 degrees and for left leg was 2.63 degrees. The peak knee external rotation at 45 cm for the right leg was 4.48 degrees and for left leg was 3.04 degrees. The peak knee external rotation at 60 cm for the right leg was 4.37 degrees and for left leg was 3.59 degrees.

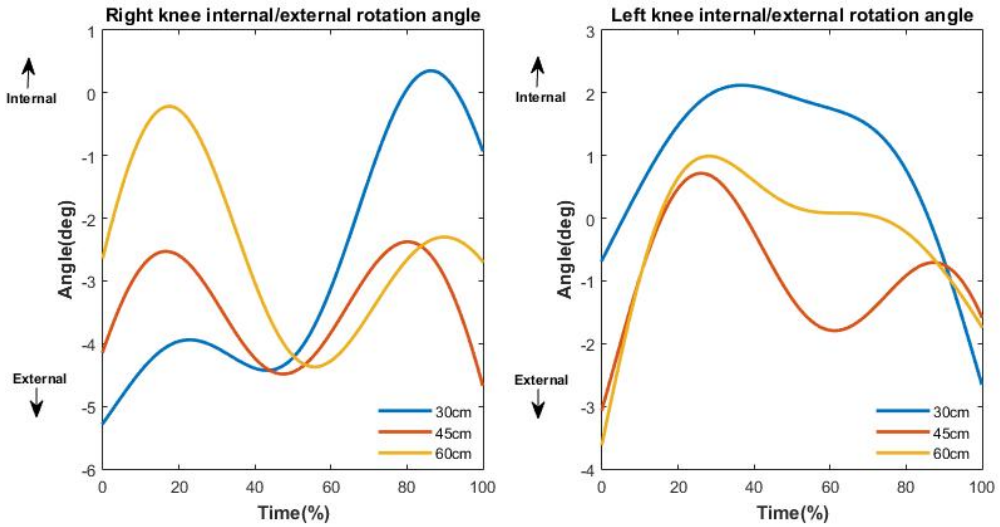

Figure 4.6: Knee external/internal rotations angles at different heights.

At the right leg the knee external rotation was higher at 30 cm. The subject landed at the initial contact with the ground with higher knee external rotation, in comparison with the others heights. It was noted that for 45 and 60 cm knee external rotation was higher after the initial contact with the ground. It is visible a reduction in external rotation as the height is increased.

In the left leg it was noted a different scenario. The maximum knee external rotation was at 60 cm at the initial contact with the ground. It was verified a reduction in knee external rotation as lower the height was. Similar results were verified relative with the work of (Bates et al., 2013) and (Mok et al., 2016) relative to drop jump at 30 cm.

According to (Berger et al., 1998) decreasing in external rotation is more suitable to the presence of lateral tracking and patellar tilt. He had verified a combined range of tibial and femoral internal rotation of (1°-4°). In addition (Dai et al., 2014) conclude that internal rotations under knee flexion angles appeared to be important risk factors for ACL injury. These range of values were verified in left leg at 30cm. This seems to be the higher risk scenario and evidence the lower integrity of the left leg in comparison with the right.

4.2.2 Kinetics

4.2.2.1 Tibiofemoral Moments

In figure 4.7 are described the Tibiofemoral moments at different heights. Through these graphs it is possible to understand the forces that are acting in the femur relative to the tibia. The moments are relative to the vertical compressive forces.

The peak TF moment at 30 cm for the right leg was 1.195 N and for left leg was 1.788 N. The peak TF moment at 45 cm for the right leg was 2.788 N and for left leg was 1.335 N. The peak TF moment at 60 cm for the right leg was 3.587 N and for left leg was 0.7128 N.

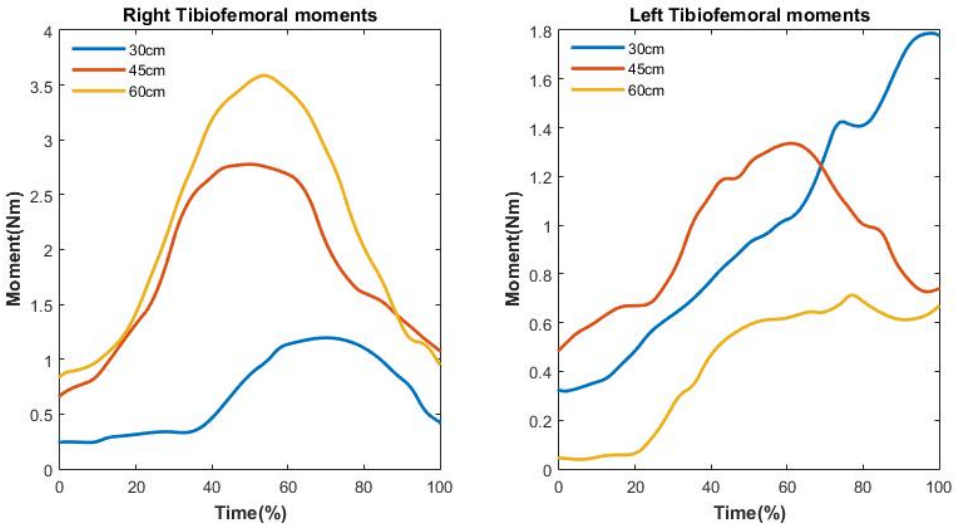

Figure 4.7: Tibiofemoral moments at different heights.

In the right leg TF moment was higher at 60 cm. In this specific trials the forces on the tibiofemoral joint were higher in comparison with the others. This could be a cause effect of higher height. In the left leg TF moment was higher at 30 cm. However, a difference was noted

relative to the other heights. This effect was relative to the peak value which occurred at the takeoff phase.

There is no much information on literature relative to tibiofemoral compressive forces on drop jumps trials. In comparison with the study of (Tsai et al., 2013) that measure compressive forces in drop jumps at 35 cm, our results have not showed much accordance. A possible reason for higher values on the right and left leg could be large compressive forces by the quadriceps as well as high activations values (Tsai et al., 2013; DeMers et al., 2014). Other explanation for TF higher moments is relative to higher knee valgus angles (Noyes et al., 2005). This effect is visible in figure 4.5 in which higher valgus were verified in the right leg at 60 cm.

4.2.2.2 Patellofemoral Moments

In figure 4.8 are described the Patellofemoral moments at different heights. Through these graphs it is possible to understand the forces that are acting in the femur relative to the patella. The moments are relative to the vertical compressive forces.

The peak PF moment at 30 cm for the right leg was 7.63 N and for left leg was 6.272 N. The peak PF moment at 45 cm for the right leg was 8.105 N and for left leg was 7.199 N. The peak PF moment at 60 cm for the right leg was 6.997 N and for left leg was 5.249 N. In both legs the PF moment was higher at 45 cm.

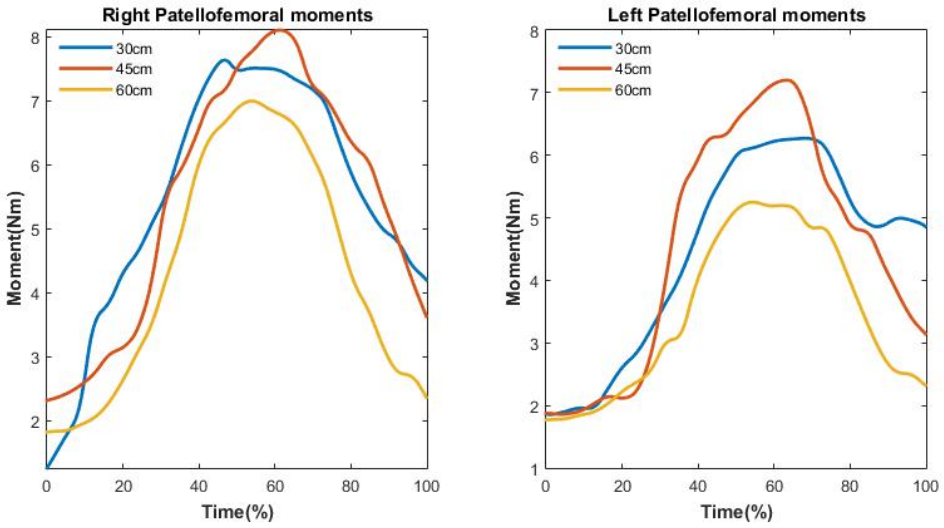

Figure 4.8: Patellofemoral Moments at different heights.

These results had some accordance with the work of (Rathleff et al., 2014). Excessive hip adduction which results in increasing of knee valgus is a reason for higher PF joint stress (Rathleff et al., 2014). In addition, abnormal femur motion relative to the tibia can increase the joint stress once decreases the patellofemoral contact area (Powers, 2010). Through the figures of hip adduction (figure 4.4) and knee valgus(figure 4.5), it could be seen that 45 cm was the higher values. In this context, the verified PF higher moments at 45 cm were justified.

4.2.2.3 Ground reaction force

In figure 4.9 are described the ground reaction forces at different heights. These graphs demonstrate the magnitude of the ground reaction forces in both legs. The peak GRF at 30 cm for the right leg was 1856 N and for left leg was 1404 N. The peak GRF at 45 cm for the right leg was 2424 N and for left leg was 1262 N. The peak GRF at 60 cm for the right leg was 2317 N and for left leg was 2069 N. These results show some accordance with the work of (Cruz et al., 2013) in which had shown that peak vertical GRF happens at 20 % of drop jump. However, it was not proven the increase on the forces as the height was increased whose was showed by (Kar, 2011).

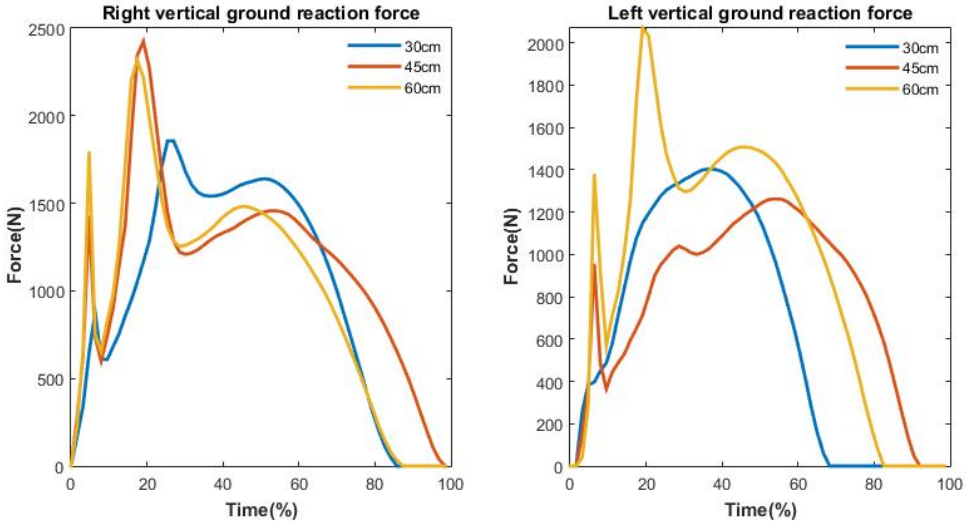

Figure 4.9: Ground reaction force at different heights.

4.2.3 Muscular analysis

4.2.3.1 ACL power

In figure 4.10 is describe the ACL power during the drop jump at different heights. In these graphs it is necessary distinct two different peaks. The negative peak means that the ACL is absorbing energy and the positive peak that ACL is giving energy to the model (Zahradnik et al., 2014).

The positive peak ACL power at 30 cm for the right leg was 43.39 W and for left leg was 24.01 W. The negative peak ACL power at 30 cm for the right leg was 47.76 W and for left leg was 46.39 W. The positive peak ACL power at 45 cm for the right leg was 48.23 wats and for left leg was 38.02 W. The negative peak ACL power at 45 cm for the right leg was 65.10 W and for left leg was 51.49 W. The positive peak ACL power at 60 cm for the right leg was 50.75 W and for left leg was 49.13 W. The negative peak ACL power at 60 cm for the right leg was 54.84 W and for left leg was 51.03 W.

Higher values of negative ACL power could compromise the ACL integrity once ACL is absorbing the energy to the capsule ligamentous (Zahradnik et al., 2014; Nyman and Armstrong,

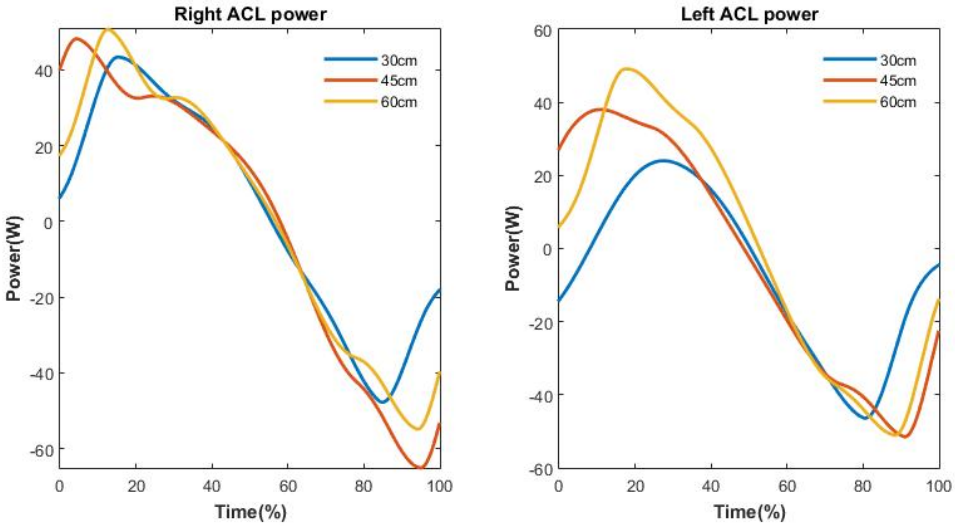

Figure 4.10: ACL power at different heights.

2015). It was verified that higher values of negative peak power were reach at the right leg at 45 cm relative to the left leg. This phenomenon could be justified once right leg was the first leg to land, and in this way it had absorbed the body height at the initial contact.

4.2.3.2 ACL length

In figure 4.11 is describe the ACL length during the drop jump at different heights. As a muscle contracts is fibre length increases in order to produce force (Brughelli and Cronin, 2007).

The peak ACL length at 30 cm for the right leg was 0.04071 m and for left leg was 0.03966 m. The peak ACL length at 45 cm for the right leg was 0.04066 m and for left leg was 0.03973 m. The peak ACL length at 60 cm for the right leg was 0.04067 m and for left leg was 0.03983 m.

It was noted that both legs had peak ACL length at initial time of the landing phase. However, there difference in the peak values. Right leg was higher values at 30 cm and left leg was higher values at 45 cm. These results are in accordance in the work of (Taylor et al., 2014) which concluded that peak ACL length occurs at when the knee flexion angle was minimal.

4.2.3.3 Activation ratios

In accordance with some research authors low (H:Q) and (G:Q) activation ratios are considered as contributors for muscular weakness which compromise knee joint integrity (Ebben et al., 2010; Kar and Quesada, 2012, 2013). In table 4.1 (H:Q) and (G:Q) activation ratios were calculated. These results are relative to the stance phase of drop jump.

It was noted that higher ratios were reached at 45 cm in both legs with the exception for H:Q at the left leg. A possible reason for this phenomenon is that low ratios are correlated with higher hip adduction and knee valgus values which was visible at 45 cm (Powers, 2010; Harput et al.,

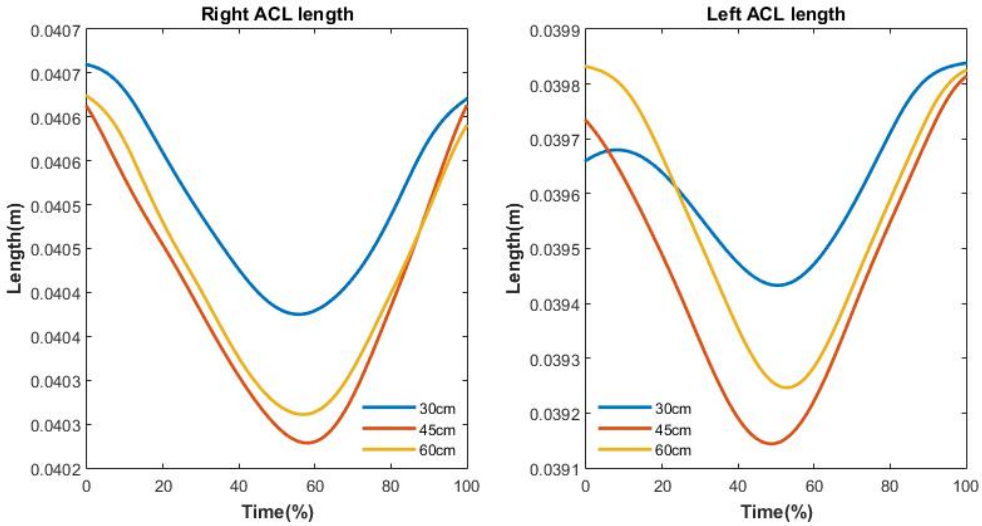

Figure 4.11: ACL fiber length at different heights.

Table 4.1: Activation ratios.

	Right		Left	
	H:Q ratio	G:Q ratio	H:Q ratio	G:Q ratio
30 cm	0,3465	1,1804	0,3738	1,2592
45 cm	0,3006	1,0148	0,5488	0,9391
60 cm	0,4442	1,4606	0,7618	1,0617

2014). Some similarity was verified with the works of (Ebben et al., 2010) and (Kar and Quesada, 2013) once the heights were a little different.

4.2.4 Overview

Through the previous analysis it was possible to identify the most dangerous jump. Drop jump at 45 cm was considered the risk jump. It was presented higher hip adduction coupled with knee valgus, low H:Q and G:Q low activation ratios. In addition, it was showed greater ACL Power and PF moments. All these variables together are considered contributors to ACL and PF injuries. In the following figures (4.12 and 4.13) it was compiled a review of kinetic, kinematic and muscle activity of this particular jump.

It was noted that peak muscle activations of hamstrings and quadriceps occurred after the peak GRF and knee flexion angle. An exception was the right bicep femoris which peaks this activation at the initial contact with the ground. Apart of this muscle, the others are in accordance with the work of (Kar and Quesada, 2012) and (Peng et al., 2011). Medial Gastrocnemius had showed high similarity with the work of (Arai et al., 2016) in drop jumps at 40 cm.

The study of quadriceps and hamstrings muscles during landing phase is very important and may allow to understand some injury scenarios. As this task involves high loads abnormal quadriceps-

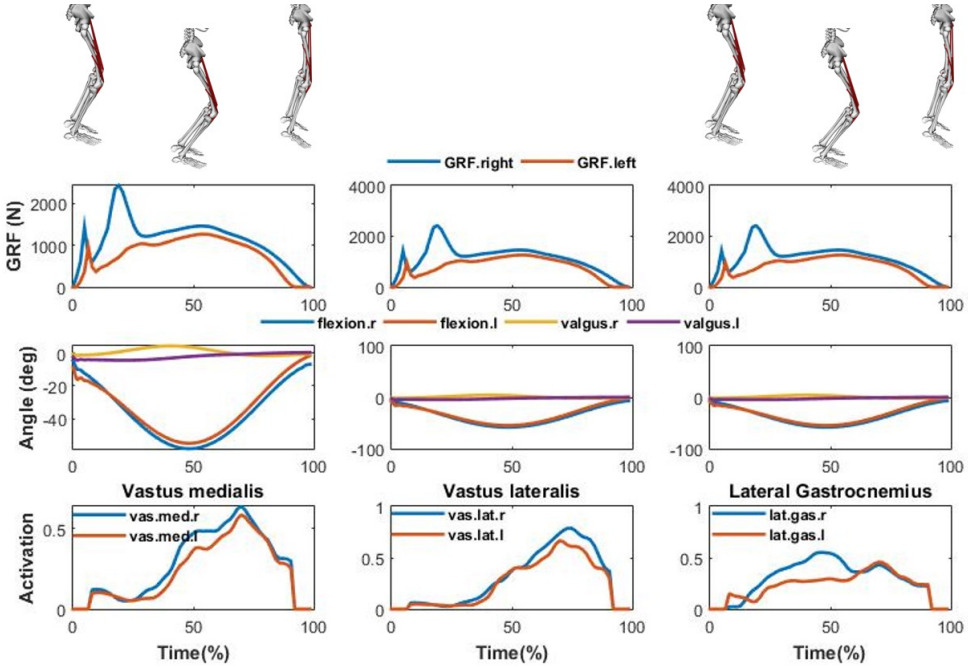

Figure 4.12: Muscular, kinematic and kinetic overview.

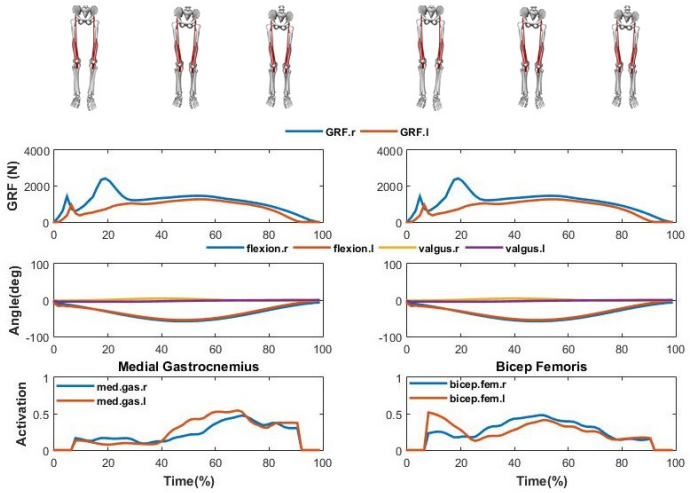

Figure 4.13: Muscular, kinematic and kinetic overview.

hamstrings activations lead to higher knee and hip valgus moments (Hewett et al., 2005a; Peng et al., 2011). In addition, low hamstrings to quadriceps activation ratios could traduce muscle weakness and high compression values from the quadriceps which compromise the stability of knee joint (Tsai et al., 2013; Harput et al., 2014).

4.3 Comparison of Healthy and Injured athlete

It was concluded previously, that drop jump at 45 cm was the most risk movement. In this context, it was changed some muscular parameters, in order to understand who an injury athlete reacts when performs a drop jump at 45 cm of height.

Activation analyses (figure 4.14) was performed at quadriceps, hamstrings, gastrocnemius muscles and ACL ligament. Through this analyse it was verified similar activations at ACL in injured and healthy athletes. An exception was high activation at the right healthy leg.

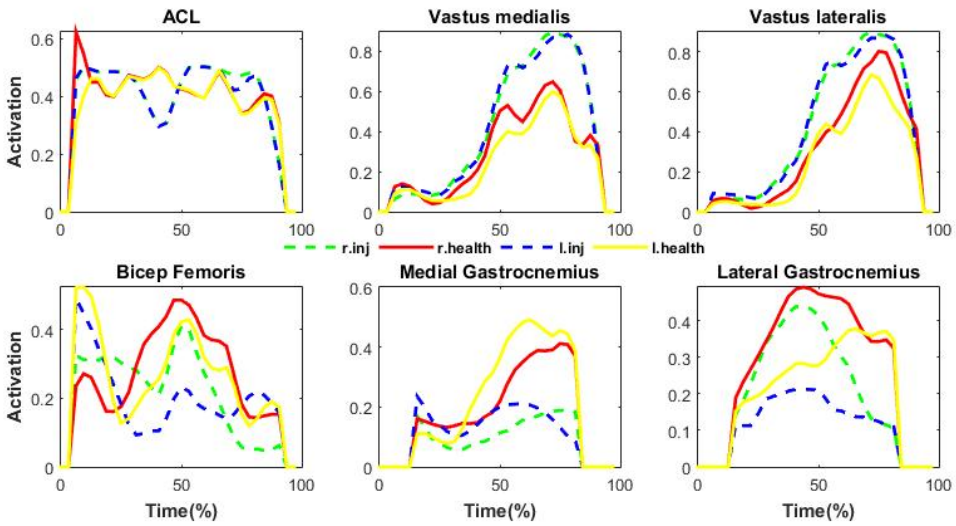

Figure 4.14: Muscle and ACL ligament activations.

Quadriceps activations showed higher activations in the injured athlete in comparison with the healthy. This phenomenon is inconsistent with the works of (Hart et al., 2010; Palmieri-smith and Villwock, 2013) which related that patients with patellofemoral pain demonstrate decreased muscular activation. A possible reason for this fact may be muscular extra activation, in order to compensate the lack of muscular force production. It was not verified a delay in the activation of vastus medialis relative to the vastus lateralis which was reported in athletes with patellofemoral disorders (Pal et al., 2014).

The obtained results had shown some accordance relative to the works of (Hewett et al., 2005a; Myer et al., 2005) during landing tasks. According to them, lateral quadriceps increasing activation leads to increased anterior shear force and ACL strain during landing. Moreover, decreased hamstrings activity combine with increased quadriceps activity may increase energy absorption

during landing which is related to ACL injury (Hewett et al., 2005a). This phenomenon is verified in the graphs of ACL power (figure 4.15a)) which showed more energy absorption by injured athletes.

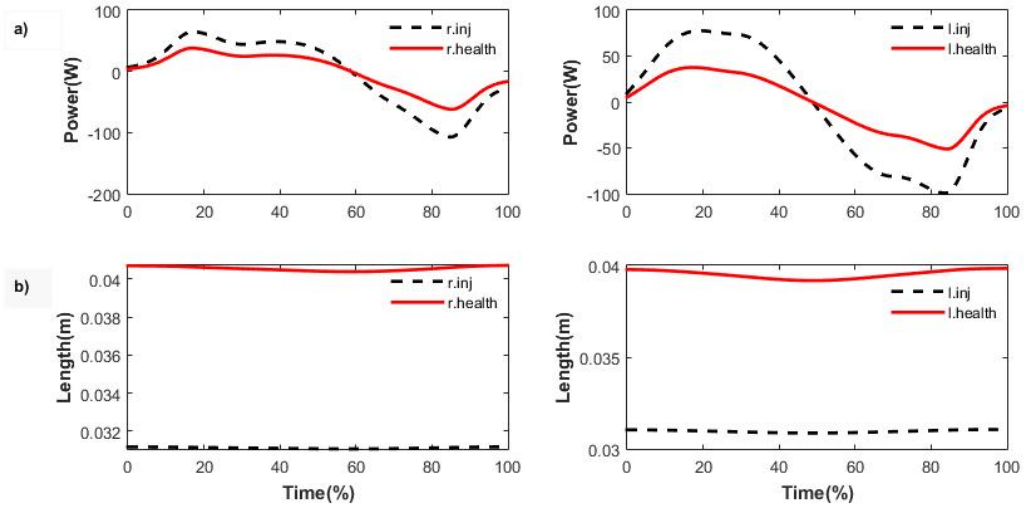

Figure 4.15: ACL power and length comparison.

Other noted occurrence was that injured subject was lower ACL fibre length , in comparison with the healthy subject (figure 4.15b)).. A possible explanation for this effect is that injured athletes contract their muscle with less muscle length in comparison with healthy athletes (Liu et al., 2012). A possible impact of this phenomenon is a drastic reduction of ACL force production illustrated in figure 4.16.

In table 4.2 is related the H:Q and G:Q activation ratios. As expected healthy athletes presented higher ration relative to the injured athletes. Moreover, and in order to improve the accuracy of this analysis it was plotted (figure 4.16) muscular forces of quadriceps and hamstrings muscle, as well as ACL ligament. Force generation of each muscle decreased in the specific strength (force/area).

Table 4.2: H:Q and G:Q activation ratios.

	Right		Left	
	H:Q ratio	G:Q ratio	H:Q ratio	G:Q ratio
Healthy	0,3006	1,0148	0,5488	0,9391
Injured	0,2853	0,4085	0,2684	0,3258

These results evidence that injured athletes show muscle weakness and quadriceps dysbalance which traduces in higher hip adduction and consequently knee valgus. In addition, lack of force production in quadriceps traduces patellar instability, once the patella is not well stabilized on the trochlear groove (Sawatsky et al., 2012). Consequently, patellar tilt and higher contact forces could be verified leading to patellofemoral joint cartilage stress resulting in pain (Petersen et al., 2014).

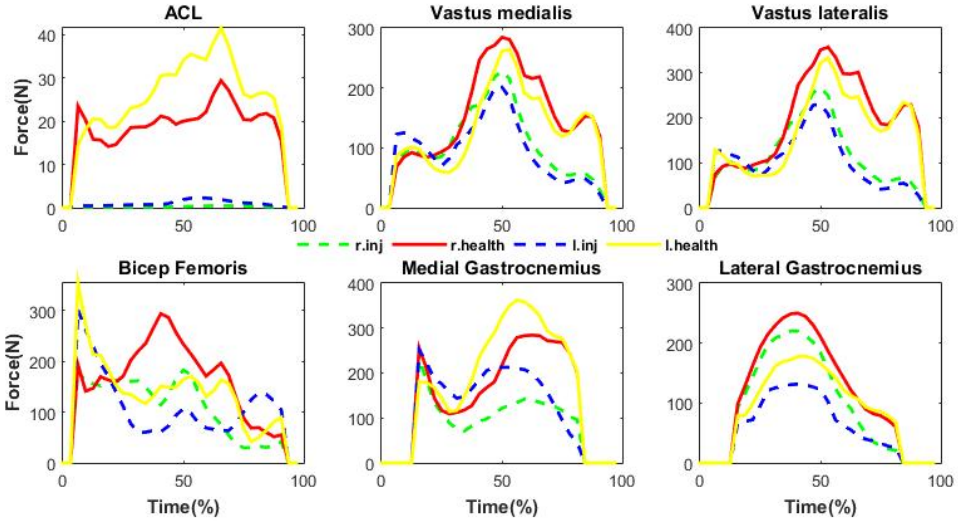

Figure 4.16: Muscle forces comparison.

4.4 Preventive programmes

Feedback trainings are emerging as a simplest and quick methodology for injury prevention and training performance (Munro et al., 2008; Munro and Herrington, 2014). The use of simple verbal feedback decreases knee valgus angles, moments, and vertical reaction forces during landing tasks according to (Munro and Herrington, 2014). Other authors believe that specific warm up programmes may reduce some lower limbs disturbances (Distefano et al., 2016). Furthermore, the use of video tapes to complement the verbal instructions is considered an efficient way to improve landing mechanism in sports movements (Munro and Herrington, 2014). In fact, ACL and patellofemoral injuries may also be decreased with specific trainings, based on hip and quadriceps muscles strengthen. Moreover, techniques based on the dissipation of the higher landing loads could also be beneficial.

4.5 Limitations

There are some limitations that should be related on this work. First, it was not used an isometric maximum voluntary contraction (MVC) method to normalize the collected EMG data. Moreover, some simplifications on musculoskeletal model were also verified. These are linked to musculoskeletal geometry. For instance, the geometry of the muscle is typically reduced to one or more line segments.

A second limitation is relative to muscle reserve actuators that act when muscle forces cannot produce force to generate movement. This reserve forces influence the Static Optimization step, in such way that is not possible to eliminate the presence of this reserves in activations and muscle forces results.

A third limitation was not to estimate bone segment geometry based on MRI images of the subject. By this way, musculoskeletal model reality would be higher as well as simulations results accuracy. At least, more knee ligaments should be introduced on the model as the Posterior cruciate ligament (PCA) and knee retinaculum.

Chapter 5

Conclusion and future work

The purpose of this study was to analyse dynamic knee variables in female athletes during drop jumps trials, in order to prevent knee injuries. These variables were relative to kinematic, kinetic and muscle data. Specifically, it was selected only the landing phase which is considered the most suitable for an injury occur.

Drop jumps simulated results showed different patterns for the different heights. A linear increasing in the variables as the heights were higher and leg symmetry was not verified. It was concluded that drop jump at 45 cm was the most dangerous trial. Indeed, it was verified higher hip adduction coupled with knee valgus, low H:Q and G:Q low activation ratios. In addition, it was showed greater ACL Power and PF moments.

Comparing injured with healthy athletes, it was visible muscle weakness and consequently lack of muscle force production. In addition, it was verified higher activations of quadriceps muscles and higher ACL energy absorption. These phenomenons had high impact on knee joint.

All these variables together are considered contributors to ACL and PF injuries. Meanwhile, hip adduction coupled with knee valgus has more impact at knee joint, once has a cause effect in the others variables.

Despite this results several future work should be done in order to access more powerful and accurate data. It is essential to perform a forward dynamic simulation. Through this simulation tool is possible to provide acceleration of joint coordinates to advance motion one step ahead in time by an integration scheme. Hence, with this tool we can change muscular parameters and then evaluate what effects this change will have in body kinematics. In addition, activation dynamics could be computed which was not verified in Static Optimization.

Furthermore, professional athletes should be integrated in this trials to evaluate their behaviour. More important, will be the analyses of the muscle fatigue that are associated to the number of games performed in a normal volleyball season. Other jumps as coutermovement and squats jumps should also be analysed.

Bibliography

F. C. Anderson and M. G. Pandy. A Dynamic Optimization Solution for Vertical Jumping in Three Dimensions. *Computer Methods in Biomechanics and Biomedical Engineering*, 2(3):201–231, 1999. ISSN 1025-5842. doi: 10.1080/10255849908907988.

F. C. Anderson and M. G. Pandy. Static and dynamic optimization solutions for gait are practically equivalent. *Journal of Biomechanics*, 34(2):153–161, 2001. ISSN 00219290. doi: 10.1016/S0021-9290(00)00155-X.

A. Arai, M. Ishikawa, and A. Ito. Agonist–antagonist muscle activation during drop jumps. *European Journal of Sport Science*, 1391(June), 2016. doi: 10.1080/17461391.2013.764930.

Basic Electronics Tutorials. ElectronicsTutorials, 2015. URL http://www.electronics-tutorials.ws/filter/filter{_}8.html.

N. A. Bates, K. R. Ford, G. D. Myer, and T. E. Hewett. Kinetic and kinematic differences between first and second landings of a drop vertical jump task : Implications for injury risk assessments . *JCLB*, 28(4):459–466, 2013. ISSN 0268-0033. doi: 10.1016/j.clinbiomech.2013.02.013. URL http://dx.doi.org/10.1016/j.clinbiomech.2013.02.013.

R. A. Berger, L. S. Crossett, J. J. Jacobs, and H. E. Rubash. Malrotation causing patellofemoral complications after total knee arthroplasty. *Clinical orthopaedics and related research*, (356): 144–153, 1998. ISSN 0009-921X. doi: 10.1097/00003086-199811000-00021.

M. J. Bey, S. K. Kline, S. Tashman, and R. Zauel. Accuracy of biplane x-ray imaging combined with model-based tracking for measuring in-vivo patellofemoral joint motion. *Journal of orthopaedic surgery and research*, 3:38, 2008. ISSN 1749-799X. doi: 10.1186/1749-799X-3-38. URL http://www.ncbi.nlm.nih.gov/pubmed/18771582.

R. W. Bisseling and A. L. Hof. Handling of impact forces in inverse dynamics. *Journal of Biomechanics*, 39(13):2438–2444, 2006. ISSN 00219290. doi: 10.1016/j.jbiomech.2005.07.021.

W. W. Briner and L. Kacmar. Common injuries in volleyball. Mechanisms of injury, prevention and rehabilitation. *Sports medicine (Auckland, N.Z.)*, 24(1):65–71, 1997. ISSN 0112-1642. doi: 10.2165/00007256-199724010-00006.

M. Brughelli and J. Cronin. Altering the Length-Tension Relationship with Eccentric Exercise Implications for Performance and Injury. *Sports Med*, 37(9):807–826, 2007.

C-Motion. Tutorial: Force Platforms, 2015. URL http://c-motion.com/v3dwiki/index.php/Tutorial:{_}Force{_}Platforms.

E. Cassell. Spiking injuries out of volleyball: a review of injury countermeasures. Technical Report 181, Monash University, 2001. URL http://www.monash.edu.au/miri/research/reports/muarc181.pdf.

P. R. Cavanagh and M. A. Lafortune. Ground reaction forces in distance running. *Journal of biomechanics*, 13(5):397–406, 1980. ISSN 0021-9290. doi: 10.1016/0021-9290(80)90033-0.

L. Chèze. Kinematic Analysis of Human Movement. *Annals of Biomedical Engineering*, 12: 144, 1984. doi: 10.1002/9781119058144. URL https://books.google.com/books?id=67pYBQAAQBAJ{&}pgis=1.

G. K. Cole, B. M. Nigg, J. L. Ronsky, and M. R. Yeadon. Application of the joint coordinate system to three-dimensional joint attitude and movement representation: a standardization proposal. *Journal of biomechanical engineering*, 115(4A):344–349, 1993. ISSN 01480731. doi: 10.1115/1.2895496.

A. Cruz, D. Bell, M. Mcgrath, T. Blackburn, D. Padua, and D. Herman. The Effects of Three Jump Landing Tasks on Kinetic and Kinematic Measures : Implications for ACL Injury Research. *Research in Sports Medicine*, (August 2014):37–41, 2013. doi: 10.1080/15438627.2013.825798.

B. Dai, D. Mao, W. E. Garrett, and B. Yu. Anterior cruciate ligament injuries in soccer: Loading mechanisms, risk factors, and prevention programs. *Journal of Sport and Health Science*, 3(4): 299–306, 2014. ISSN 22132961. doi: 10.1016/j.jshs.2014.06.002. URL http://dx.doi.org/10.1016/j.jshs.2014.06.002.

S. L. Delp, J. P. Loan, M. G. Hoy, F. E. Zajac, E. L. Topp, and J. M. Rosen. An Interactive Graphics-Based Model of the Lower Extremity to Study Orthopaedic Surgical Procedures, 1990. ISSN 15582531.

S. L. Delp, F. C. Anderson, A. S. Arnold, P. Loan, A. Habib, C. T. John, E. Guendelman, and D. G. Thelen. OpenSim: Open-source software to create and analyze dynamic simulations of movement. *IEEE Transactions on Biomedical Engineering*, 54(11):1940–1950, 2007. ISSN 00189294. doi: 10.1109/TBME.2007.901024.

M. S. DeMers, S. Pal, and S. L. Delp. Changes in tibiofemoral forces due to variations in muscle activity during walking. *Journal of Orthopaedic Research*, 32(6):769–776, 2014. ISSN 1554527X. doi: 10.1002/jor.22601.

L. J. Distefano, S. W. Marshall, D. A. Padua, K. Y. Peck, A. I. Beutler, S. J. D. Motte, B. S. Frank, J. C. Martinez, K. L. Cameron, L. J. Distefano, and S. W. Marshall. The American Journal of Sports Medicine The Effects of an Injury Prevention Program on Landing Biomechanics Over Time. *The American Journal Of Sports Medicine*, 2016. doi: 10.1177/0363546515621270.

A. V. Dowling, J. Favre, and T. P. Andriacchi. Inertial Sensor-Based Feedback Can Reduce Key Risk Metrics for Anterior Cruciate Ligament Injury During Jump Landings. *The American Journal of Sports Medicine*, 40(5):1075–1083, 2012. ISSN 0363-5465. doi: 10.1177/0363546512437529. URL http://journal.ajsm.org/cgi/doi/10.1177/0363546512437529.

W. Ebben, M. Fauth, E. Petushek, L. Garceu, and B. Hsu. Gender-Based Analysis of Hamstring and Quadriceps Muscle Activation During Jump Landings and Cutting. *Journal of Strength and Conditioning Research*, 24(2):408–415, 2010.

F. D. Farfán, J. C. Politti, and C. J. Felice. Evaluation of EMG processing techniques using Information Theory. *Biomedical engineering online*, 9:72, 2010. ISSN 1475-925X. doi: 10.1186/1475-925X-9-72.

J. Favre, R. Aissaoui, B. Jolles, J. de Guise, and K. Aminian. Functional calibration procedure for 3D knee joint angle description using inertial sensors. *Journal of Biomechanics*, 42(14):2330–2335, 2009. ISSN 00219290. doi: 10.1016/j.jbiomech.2009.06.025. URL http://linkinghub.elsevier.com/retrieve/pii/S0021929009003649.

F. Feldhege, A. Mau-Moeller, T. Lindner, A. Hein, A. Markschies, U. Zettl, and R. Bader. Accuracy of a Custom Physical Activity and Knee Angle Measurement Sensor System for Patients with Neuromuscular Disorders and Gait Abnormalities. *Sensors*, 15(5):10734–10752, 2015. ISSN 1424-8220. doi: 10.3390/s150510734. URL http://www.mdpi.com/1424-8220/15/5/10734/.

R. Ferber, K. D. Kendall, and L. Farr. Changes in knee biomechanics after a hip-abductor strengthening protocol for runners with patellofemoral pain syndrome. *Journal of Athletic Training*, 46(2):142–149, 2011. ISSN 10626050. doi: 10.4085/1062-6050-46.2.142.

A. Ferretti, P. Papandrea, F. Conteduca, and P. P. Mariani. Knee ligament injuries in volleyball players. *The American Journal of Sports Medicine*, 20(2):203–207, 1992. ISSN 0363-5465. doi: 10.1177/036354659202000219.

F. Flandry and G. Hommel. Normal anatomy and biomechanics of the knee. *Sports medicine and arthroscopy review*, 19(2):82–92, 2011. ISSN 1062-8592. doi: 10.1097/JSA.0b013e318210c0aa.

J. P. Fulkenson. *Disorders of the Patellofemoral Joint*. Lippincott Williams and Wilkins, Philadelphia, 4th edition, 2004.

P. Gerus, M. Sartori, T. F. Besier, B. J. Fregly, S. L. Delp, S. A. Banks, M. G. Pandy, D. D. D'Lima, and D. G. Lloyd. Subject-specific knee joint geometry improves predictions of medial tibiofemoral contact forces. *Journal of Biomechanics*, 46(16):2778–2786, 2013. ISSN 00219290. doi: 10.1016/j.jbiomech.2013.09.005. URL http://dx.doi.org/10.1016/j.jbiomech.2013.09.005.

A. Godfrey, R. Conway, D. Meagher, and G. ÓLaighin. Direct measurement of human movement by accelerometry. *Medical Engineering and Physics*, 30(10):1364–1386, 2008. ISSN 13504533. doi: 10.1016/j.medengphy.2008.09.005.

A. Golant, T. Quach, and J. Rosen. Patellofemoral Instability : Diagnosis and Management Ch. *Current Issues in Sports and Exercise Medicine*, 2013.

F. D. Groote, I. Jonkers, L. Modenese, M. Sartori, G. Valente, and M. Wesseling. Advance your projects in musculoskeletal modeling and simulation of movement using OpenSim. In O. Documentation, editor, *OpenSim Europe Workshop Bologna*, Bologna, 2016.

S. R. Hamner, A. Seth, and S. L. Delp. Muscle contributions to propulsion and support during running. *Journal of Biomechanics*, 43(14):2709–2716, 2010. ISSN 00219290. doi: 10.1016/j.jbiomech.2010.06.025. URL http://dx.doi.org/10.1016/j.jbiomech.2010.06.025.

G. Harput, A. R. Soylu, H. Ertan, N. Ergun, and C. G. Mattacola. Effect of Gender on the Quadriceps-to-Hamstrings Coactivation Ratio During Different Exercises. *Journal of Sports Reabilitation*, pages 36–43, 2014.

J. M. Hart, B. Pietrosimone, J. Hertel, and C. D. Ingersoll. Quadriceps Activation Following Knee Injuries :. *Journal of Athletic Training*, 45(1):87–97, 2010.

S. Heintz. *Muscular Forces from Static Optimization*. PhD thesis, 2006.

T. E. Hewett, G. D. Myer, and K. R. Ford. Biomechanical Measures of Neuromuscular Control and Valgus Loading of the Knee Predict Anterior Cruciate Ligament Injury Risk in Female Athletes. *Mechanical Engineering Department at EngagedScholarship@CSU*, 33(4):492–501, 2005a.

T. E. Hewett, B. T. Zazulak, G. D. Myer, and K. R. Ford. A review of electromyographic activation levels, timing differences, and increased anterior cruciate ligament injury incidence in female athletes. *British journal of sports medicine*, pages 347–351, 2005b. doi: 10.1136/bjsm.2005.018572.

J. Hicks. Confluence - OpenSim Documentation, 2012. URL http://simtk-confluence.stanford.edu:8080/display/OpenSim/OpenSim+Support.

J. L. Hicks, T. K. Uchida, A. Seth, A. Rajagopal, and S. Delp. Is my model good enough? Best practices for verification and validation of musculoskeletal models and simulations of human movement. *Journal of Biomechanical Engineering*, 137(February):020905, 2015. ISSN 1528-8951. doi: 10.1115/1.4029304.

M. Z. Jamal. Signal Acquisition Using Surface EMG and Circuit Design Considerations for Robotic Prosthesis. 2012. doi: 10.5772/52556.

S. v. S. Jan. *Color Atlas of Skeletal Landmark Definitions: Guidelines for Reproducible Manual and Virtual Palpations*. Churchill Livingstone, 2007.

J. Kar. *A forward dynamics simulation study of increasing load on the anterior cruciate ligament of the k ...* PhD thesis, University of Louisville, 2011.

J. Kar and P. M. Quesada. A Numerical Simulation Approach to Studying Anterior Cruciate Ligament Strains and Internal Forces Among Young Recreational Women Performing Valgus Inducing Stop-Jump Activities. *Annals of Biomedical Engineering*, 40(8):1679–1691, 2012. ISSN 0090-6964. doi: 10.1007/s10439-012-0572-x. URL http://link.springer.com/10.1007/s10439-012-0572-x.

J. Kar and P. M. Quesada. A musculoskeletal modeling approach for estimating anterior cruciate ligament strains and knee anterior-posterior shear forces in stop-jumps performed by young recreational female athletes. *Annals of biomedical engineering*, 41(2):338–48, 2013. ISSN 1573-9686. doi: 10.1007/s10439-012-0644-y. URL http://www.ncbi.nlm.nih.gov/pubmed/23015067.

A. G. Kirk, J. F. O'Brien, and D. a. Forsyth. Skeletal parameter estimation from optical motion capture data. *IEEE Computer Society Conference on Computer Vision and Pattern Recognition*, 2:782–788, 2005. ISSN 1063-6919. doi: 10.1109/CVPR.2005.326.

H. Kreder and G. Hawker. The knee. In *Fam's Musculoskeletal Examination and Joint Injection Techniques (Second Edition)*, chapter The Knee, pages 65–88. 2010. doi: 10.1016/B978-1-4160-5595-2.00022-5.

T. Krosshaug, A. Nakamae, B. P. Boden, L. Engebretsen, G. Smith, J. R. Slauterbeck, T. E. Hewett, and R. Bahr. Mechanisms of anterior cruciate ligament injury in basketball: video analysis of 39 cases. *The American journal of sports medicine*, 35(3):359–67, mar 2007. ISSN 0363-5465. doi: 10.1177/0363546506293899. URL http://www.ncbi.nlm.nih.gov/pubmed/17092928.

K. Kurihara, S. Hoshino, K. Yamane, and Y. Nakamura. Optical motion capture system with pan-tilt camera tracking and\nreal time data processing. *Proceedings 2002 IEEE International Conference on Robotics and Automation (Cat. No.02CH37292)*, 2:1241–1248, 2002. ISSN 10504729. doi: 10.1109/ROBOT.2002.1014713. URL http://nobunaga.t.u-tokyo.ac.jp/publications/pdf2002/icra02/kurihara.pdf.

Z. F. Lerner, M. S. DeMers, S. L. Delp, and R. C. Browning. How tibiofemoral alignment and contact locations affect predictions of medial and lateral tibiofemoral contact forces. *Journal of Biomechanics*, 48(4):644–650, 2015. ISSN 18732380. doi: 10.1016/j.jbiomech.2014.12.049. URL http://dx.doi.org/10.1016/j.jbiomech.2014.12.049.

Y.-C. Lin, T. W. Dorn, A. G. Schache, and M. G. Pandy. Comparison of different methods for estimating muscle forces in human movement. *Proceedings of the Institution of Mechanical Engineers, Part H: Journal of Engineering in Medicine*, 226(2):103–112, 2011. ISSN 0954-4119. doi: 10.1177/0954411911429401. URL http://pih.sagepub.com/lookup/doi/10.1177/0954411911429401$\delimiter"026E30F$nhttp://pih.sagepub.com/content/226/2/103.abstract.

H. Liu, W. E. Garrett, C. T. Moorman, and B. Yu. Injury rate, mechanism, and risk factors of hamstring strain injuries in sports: A review of the literature. *Journal of Sport and Health Science*, 1(2):92–101, 2012. ISSN 20952546. doi: 10.1016/j.jshs.2012.07.003. URL http://www.sciencedirect.com/science/article/pii/S2095254612000452.

B. Malfait, B. Dingenen, A. Smeets, F. Staes, T. Pataky, A. Robinson, J. Vanrenterghem, and S. Verschueren. Knee and Hip Joint Kinematics Predict Quadriceps and Hamstrings Neuromuscular Activation Patterns in Drop Jump Landings. *PLOS ONE*, pages 1–18, 2016. doi: 10.1371/journal.pone.0153737.

J. J. Mason, F. Leszko, T. Johnson, and R. D. Komistek. Patellofemoral joint forces. *Journal of biomechanics*, 41(11):2337–48, aug 2008. ISSN 0021-9290. doi: 10.1016/j.jbiomech.2008.04.039. URL http://www.ncbi.nlm.nih.gov/pubmed/18644310.

R. Merletti and P. J. Parker. *Electromyography: Physiology, Engineering, and Noninvasive Applications*. 2004. ISBN 3175723993.

M. Millard, T. Uchida, A. Seth, and S. L. Delp. Flexing computational muscle: modeling and simulation of musculotendon dynamics. *J Biomech Eng*, 135(2):21005, 2013. ISSN 1528-8951. doi: 10.1115/1.4023390. URL http://www.ncbi.nlm.nih.gov/pubmed/23445050$\delimiter"026E30F$nhttp://biomechanical.asmedigitalcollection.asme.org/article.aspx?articleid=1666657$\delimiter"026E30F$nhttp://www.pubmedcentral.nih.gov/articlerender.fcgi?artid=3705831{&}tool=pmcentrez{&}rendertype=abstract.

K.-m. Mok, T. D. If, E. Petushek, and T. Krosshaug. Gait & Posture Reliability of knee biomechanics during a vertical drop jump in elite female athletes. *Gait & Posture*, 46:173–178, 2016. ISSN 0966-6362. doi: 10.1016/j.gaitpost.2016.03.003. URL http://dx.doi.org/10.1016/j.gaitpost.2016.03.003.

A. Munro and L. Herrington. The effect of videotape augmented feedback on drop jump landing strategy: Implications for anterior cruciate ligament and patellofemoral joint injury prevention.

The Knee, 2014. ISSN 0968-0160. doi: 10.1016/j.knee.2014.05.011. URL http://dx.doi.org/10.1016/j.knee.2014.05.011.

B. J. Munro, T. E. Campbell, G. G. Wallace, and J. R. Steele. The intelligent knee sleeve: A wearable biofeedback device. *Sensors and Actuators, B: Chemical*, 131(2):541–547, 2008. ISSN 09254005. doi: 10.1016/j.snb.2007.12.041.

G. D. Myer, K. R. Ford, and T. E. Hewett. The effects of gender on quadriceps muscle activation strategies during a maneuver that mimics a high ACL injury risk position. *Journal of Electromyography and Kinesiology*, 15:181–189, 2005. doi: 10.1016/j.jelekin.2004.08.006.

F. R. Noyes, S. D. Barber-westin, C. Fleckenstein, C. Walsh, and J. West. The Drop-Jump Screening Test Difference in Lower Limb Control By Gender and Effect of Neuromuscular Training in Female Athletes. *The American Journal Of Sports Medicine*, pages 197–207, 2005. doi: 10.1177/0363546504266484.

E. Nyman and C. W. Armstrong. Real-Time Feedback During Drop Landing Training Improves Subsequent Frontal and Sagittal Plane Knee Kinematics. *Clinical Biomechanics*, 2015. ISSN 02680033. doi: 10.1016/j.clinbiomech.2015.06.018. URL http://www.sciencedirect.com/science/article/pii/S0268003315001825.

D. R. Ortega, E. C. Rodríguez Bíes, and F. J. Berral de la Rosa. Analysis of the vertical ground reaction forces and temporal factors in the landing phase of a countermovement jump. *Journal of Sports Science and Medicine*, 9(March):282–287, 2010. ISSN 13032968.

S. Pal, T. Besier, G. Beaupre, M. Fredericson, S. Delp, and G. Gold. Patellar maltracking is prevalent among patellofemoral pain subjects with patella alta: an upright, weightbearing MRI study. *Orthop Res.*, 31(3):448–457, 2014. doi: 10.1002/jor.22256.Patellar.

R. M. Palmieri-smith and M. Villwock. Pain and Effusion and Quadriceps Activation and Strength. *Journal of Athletic Training*, 48(2):186–191, 2013. doi: 10.4085/1062-6050-48.2.10.

H.-t. Peng, T. W. Kernozek, and C.-y. Song. Physical Therapy in Sport Quadricep and hamstring activation during drop jumps with changes in drop height. *Physical Therapy in Sport*, 12(3): 127–132, 2011. ISSN 1466-853X. doi: 10.1016/j.ptsp.2010.10.001. URL http://dx.doi.org/10.1016/j.ptsp.2010.10.001.

W. Petersen, A. Ellermann, A. Koppenbur, R. Best, I. Rembitzki, G. Bruggemam, and C. Liebau. Patellofemoral pain syndrome ¨. *Knee Surg Sports Traumotol Arthrose*, pages 2264–2274, 2014. doi: 10.1007/s00167-013-2759-6.

C. M. Powers. Clinical commentary Hip Mechanics on Knee Injury: A Biomechanical Perspective. *Journal Of Orthopaedic Sports Physical Therapy*, 40(2):42–51, 2010. doi: 10.2519/jospt.2010.3337.

M. S. Rathleff, C. Richter, C. Brushoj, J. Bencke, T. Brandholm, P. Holmich, and K. Thorborg. Increased medial foot loading during drop jump in subjects with patellofemoral pain. *Knee Surg Sports Traumatol Arthose*, 2014. doi: 10.1007/s00167-014-2943-3.

J. C. Reeser and R. Bahr. Principles of prevention and treatment of common volleyball injuries. *FIVB Medical Commission*, 2011.

J. A. Reinbolt, A. Seth, and S. L. Delp. Simulation of human movement: applications using OpenSim. *Procedia IUTAM*, 2:186–198, 2011. ISSN 22109838. doi: 10.1016/j.piutam.2011.04.019. URL http://linkinghub.elsevier.com/retrieve/pii/S2210983811000204.

D. G. E. Robertson and J. J. Dowling. Design and responses of Butterworth and critically damped digital filters. *Journal of Electromyography and Kinesiology*, 13(6):569–573, 2003. ISSN 10506411. doi: 10.1016/S1050-6411(03)00080-4.

A. Sawatsky, D. Bourne, M. Horisberger, A. Jinha, and W. Herzog. Changes in patellofemoral joint contact pressures caused by vastus medialis muscle weakness. *Clinical Biomechanics*, 27 (6):595–601, 2012. ISSN 02680033. doi: 10.1016/j.clinbiomech.2011.12.011. URL http://dx.doi.org/10.1016/j.clinbiomech.2011.12.011.

C. Schönauer, T. Pintaric, and H. Kaufmann. A Flexible Marker-Based Solution. 2011.

T. Seel, J. Raisch, and T. Schauer. IMU-Based Joint Angle Measurement for Gait Analysis. *Sensors*, 14(4):6891–6909, 2014. ISSN 1424-8220. doi: 10.3390/s140406891. URL http://www.mdpi.com/1424-8220/14/4/6891/.

R. Seeley, T. Stephens, and P. Tate. *Seeley's Anatomy & Physiology*. McGraw-Hill, 2005. ISBN 972-8930-07-0.

A. Seth, M. Sherman, J. a. Reinbolt, and S. L. Delp. OpenSim: A musculoskeletal modeling and simulation framework for in silico investigations and exchange. *Procedia IUTAM*, 2:212–232, 2011. ISSN 22109838. doi: 10.1016/j.piutam.2011.04.021. URL http://dx.doi.org/10.1016/j.piutam.2011.04.021.

S. Shalhoub and L. P. Maletsky. Variation in patellofemoral kinematics due to changes in quadriceps loading configuration during in vitro testing. *Journal of Biomechanics*, 47(1):130–136, 2014. ISSN 00219290. doi: 10.1016/j.jbiomech.2013.09.019. URL http://dx.doi.org/10.1016/j.jbiomech.2013.09.019.

S. L. Sherman, A. C. Plackis, and C. W. Nuelle. Patellofemoral anatomy and biomechanics. *Clinics in Sports Medicine*, 33(3):389–401, 2014. ISSN 1556228X. doi: 10.1016/j.csm.2014.03.008. URL http://dx.doi.org/10.1016/j.csm.2014.03.008.

P. B. Shull, W. Jirattigalachote, M. a. Hunt, M. R. Cutkosky, and S. L. Delp. Quantified self and human movement: a review on the clinical impact of wearable sensing and feedback for gait analysis and intervention. *Gait & posture*, 40(1):11–9, may 2014. ISSN 1879-2219. doi: 10.1016/j.gaitpost.2014.03.189. URL http://www.ncbi.nlm.nih.gov/pubmed/24768525.

K. Singhal, J. Kim, J. Casebolt, S. Lee, K.-H. Han, and Y.-H. Kwon. Gender difference in older adult's utilization of gravitational and ground reaction force in regulation of angular momentum during stair descent. *Human Movement Science*, 41:230–239, 2015. ISSN 0167-9457. doi: 10.1016/j.humov.2015.03.004. URL 10.1016/j.humov.2015.03.004$\delimiter"026E30F$nhttp://0-search.ebscohost.com.opac.lib.ntnu.edu.tw/login.aspx?direct=true{&}db=edselp{&}AN=S0167945715000469{&}lang=zh-tw{&}site=eds-live.

R. B. Souza and C. M. Powers. Differences in hip kinematics, muscle strength, and muscle activation between subjects with and without patellofemoral pain. *The Journal of orthopaedic and sports physical therapy*, 39(1):12–9, 2009. ISSN 0190-6011. doi: 10.2519/jospt.2009.2885. URL http://www.ncbi.nlm.nih.gov/pubmed/19131677.

K. M. Steele, M. S. DeMers, M. H. Schwartz, and S. L. Delp. Compressive tibiofemoral force during crouch gait. *Gait and Posture*, 35(4):556–560, 2012. ISSN 09666362. doi: 10.1016/j.gaitpost.2011.11.023. URL http://dx.doi.org/10.1016/j.gaitpost.2011.11.023.

K. A. Taylor, H. C. Cutcliffe, R. M. Queen, G. M. Utturkar, C. E. Spritzer, W. E. Garret, and L. E. DeFrate. In vivo measurement of ACL length and relative strain during walking. *Journal of Biomechanics*, 46(3):478–483, 2014. doi: 10.1016/j.jbiomech.2012.10.031.In.

T. Taylor. Knee joint, 2015. URL http://www.innerbody.com/image/skel16.html{#}full-description.

D. G. Thelen. Adjustment of muscle mechanics model parameters to simulate dynamic contractions in older adults. *Journal of biomechanical engineering*, 125(1):70–77, 2003. ISSN 01480731. doi: 10.1115/1.1531112.

S. Thomas, D. Rupiper, and G. S. Stacy. Imaging of the Patellofemoral Joint. *Clinics in Sports Medicine*, 33(3):413–436, 2014. ISSN 02785919. doi: 10.1016/j.csm.2014.03.007. URL http://linkinghub.elsevier.com/retrieve/pii/S0278591914000246.

L.-c. Tsai, I. S. Scher, and C. M. Powers. Quantification of Tibiofemoral Shear and Compressive Loads Using an MRI-Based EMG-Driven Knee Model. *Journal of Applied Biomechanics*, (1): 229–234, 2013.

J. J. C. van den Noort, M. van der Esch, M. P. M. Steultjens, J. Dekker, M. H. M. Schepers, P. H. Veltink, and J. Harlaar. Ambulatory measurement of the knee adduction moment in patients with osteoarthritis of the knee. *Journal of biomechanics*, 46(1):43–9, 2013. ISSN 1873-2380. doi: 10.1016/j.jbiomech.2012.09.030. URL http://www.sciencedirect.com/science/article/pii/S0021929012005817.

N. Vlietstra. *Comparing Methods for Full Body Inverse Dynamics Analysis of a Standing Long Jump*. PhD thesis, Grand Valley State University, 2014.

N. a. Wilson, J. M. Press, J. L. Koh, R. W. Hendrix, and L.-Q. Zhang. In vivo noninvasive evaluation of abnormal patellar tracking during squatting in patients with patellofemoral pain. *The Journal of bone and joint surgery. American volume*, 91(3):558–566, 2009. ISSN 0021-9355. doi: 10.2106/JBJS.G.00572.

H. Xu, D. Bloswick, and A. Merryweather. An improved OpenSim gait model with multiple degrees of freedom knee joint and knee ligaments. *Comput Methods Biomech Biomed Engin*, 2015.

F. Yu and Q. Sun. Angular rate optimal design for the rotary strapdown inertial navigation system. *Sensors (Basel, Switzerland)*, 14(4):7156–80, 2014. ISSN 1424-8220. doi: 10.3390/s140407156. URL http://www.pubmedcentral.nih.gov/articlerender.fcgi?artid=4029711{&}tool=pmcentrez{&}rendertype=abstract.

D. Zahradnik, D. Jandacka, J. Uchytil, R. Farana, and J. Hamill. Lower extremity mechanics during landing after a volleyball block as a risk factor for anterior cruciate ligament injury. *Physical Therapy in Sport*, 16(1):53–58, 2014. ISSN 1466853X. doi: 10.1016/j.ptsp.2014.04.003. URL http://dx.doi.org/10.1016/j.ptsp.2014.04.003.

F. E. Zajac. Muscle and tendon: properties, models, scaling, and application to biomechanics and motor control., 1989. ISSN 0278-940X.

Appendix A

Model properties

In table A.1 and figure A.1 it is represented the standard values of the gait2392 model. Through these values our model was scaled, in order to match the subject characteristics and anthropometry.

Table A.1: Model parameters.

Body Segments		**Moments of inertia**		
		xx	**yy**	**zz**
Torso	34,2366	1,4745	0,7555	1,4314
Pelvis	11,777	0,1028	0,0871	0,0579
Right femur	9,3014	0,1339	0,0351	0,1412
Right tibia	3,7075	0,0504	0,0051	0,0511
Right patella	0,0862	0,00000287	0,00001311	0,00001311
Right talus	0,1000	0,0010	0,0010	0,0010
Right calcaneus	1,250	0,0014	0,0039	0,0041
Right toe	0,2166	0,0001	0,0002	0,0010
Left femur	9,3014	0,1339	0,0351	0,1412
Left tibia	3,7075	0,0504	0,0051	0,0511
Left patella	0,0862	0,00000287	0,00001311	0,00001311
Left talus	0,1000	0,0010	0,0010	0,0010
Left calcaneus	1,250	0,0014	0,0039	0,0041
Left toe	0,2166	0,0001	0,0002	0,0010

joint / type		muscle	Gait2392 max isometric force (N)
HIP	flex, abd, inrot	glut_med_1	819
	abd	glut_med_2	573
	ext, abd, exrot	glut_med_3	653
	flex, abd, inrot	glut_min_1	270
	abd	glut_min_2	285
	ext, abd, exrot	glut_min_3	323
	ext, abd	glut_max_1	573
	ext	glut_max_2	819
	ext	glut_max_3	552
	flex, ext(?), add	add_long	627
	flex, add	add_brev	429
	flex, add	pect	266
	exrot	quad_fem	381
	exrot	gem	164
	abd, exrot	piriformis	444
	ext, add	add_mag_1	381
	ext, add	add_mag_2	343
	ext, add	add_mag_3	488
	flex, inrot	iliacus	1073
	flex, inrot	psoas	1113
HIP/KNEE	h_flex, k_ext	rect_fem	1169
	h_flex, h_add, k_flex	gracilis	162
	h_flex, h_abd, k_flex	sartorius	156
	h_flex, h_abd, h_inrot	tfl	233
	h_ext, h_add, k_flex	semimem	1288
	h_ext, h_add, k_flex	semiten	410
	h_ext, h_add, k_flex	bi_fem_lh	896
KNEE	ext	vast_med	1294
	ext	vast_int	1365
	ext	vast_lat	1871
	flex	bi_fem_sh	804
KNEE/ANKLE	k_flex, a_pf	med_gas	1558
	k_flex, a_pf	lat_gas	683
ANKLE	pf, ev	per_brev	435
	pf, ev	per_long	943
	pf	soleus	3549
	pf, inv	tib_post	1588
	pf, inv	fl_dig_long	310
	pf, inv	fl_hal_long	322
	df, inv	tib_ant	905
	df, ev	ext_dig_long	512
	df, inv	ext_hal_long	162
	df, ev	per_tert	180

Figure A.1: Maximum isometric force of the muscles on the model.

Appendix B

Athlete consent

In figure B.1 is illustrated the consent signed by the female athlete on these trials.

U.PORTO

UNIVERSIDADE DO PORTO

Declaração de consentimento informado

Tarefa de aquisição de dados de movimento e Electromiográficos

Eu, abaixo assinado, Ana Catarina Soares Martins, compreendi a explicação que me foi fornecida acerca do estudo " Simulação Biomecânica em atletas de voleibol no movimento Drop Jump " para a recolha de dados relativos ao movimento Drop Jump em que irei participar tendo-me sido dado a oportunidade de fazer as perguntas que julguei necessárias e, de todas, obtive resposta satisfatória.

Foi me também explicado os objetivos do estudo, os benefícios previstos e eventuais situações de risco e desconforto.

Além disso, foi-me informado que tenho o direito de recusar a todo o tempo a minha participação no estudo. Os registos dos resultados poderão ser consultados pelos responsáveis científicos e ser objeto de publicação, mas os elementos da identidade pessoal serão sempre tratados de modo estritamente confidencial.

Por isso, consinto participar respondendo a todas as questões propostas pelo investigador.

PORTO, 29 de MARÇO de 2016

Assinatura do participante:

Ana Martins

Assinatura do investigador responsável:

João Cunha

Figure B.1: Consent document